LA-UR-16-23458
Approved for public release; distribution is unlimited.

Title: Determination of the Spectral Index in the Fission Spectrum Energy Regime

Author(s): Lee, Amy Sarah

Intended for: Report

Issued: 2016-05-16

(U) Determination of the Spectral Index in the Fission Spectrum Energy Regime

A.S. Lee
C-NR
May 12, 2016
LA-UR

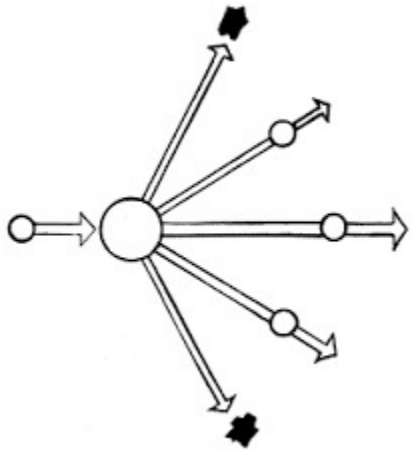

Los Alamos
NATIONAL LABORATORY
P.O. BOX 1663
Los Alamos, NM 87544

[With the exception of this statement, the page number and the classification markings, this page was intentionally left blank.]

Determination of the Spectral Index in the Fission Spectrum Energy Regime

by
A.S. Lee

May 12, 2016

— 1 — Introduction

Neutron reaction cross sections play a vital role in tracking the production and destruction of isotopes exposed to neutron fluence. They are central to the process of reconciling the initial and final atom inventories. Measurements of irradiated samples by radiochemical methods in tangent with an algorithm are used to evaluate the fluence a sample is exposed to over the course of the irradiation. This algorithm is the Isotope Production Code (IPC) created and used by the radiochemistry data assessment team at Los Alamos National Laboratory (LANL). An integral result is calculated by varying the total neutron fluence seen by a sample. A sample, irradiated in a critical assembly, will be exposed to a unique neutron flux defined by the neutron source and distance of the sample from the source. Neutron cross sections utilized are a function of the hardness of the neutron spectrum at the location of irradiation. A spectral index is used an indicator of the hardness of the neutron spectrum. Cross sections fit forms applied in IPC are collapsed from a LANL 30-group energy structure. Several decades of research and development have been performed to formalize the current IPC cross section library. Basis of the current fission spectrum neutron reaction cross section library is rooted in critical assembly experiments performed from the 1950's through the early 1970's at LANL. The focus of this report is development of the spectral index used an indicator of the hardness of the neutron spectrum in the fission spectrum energy regime.

— 2 — Algorithm Overview

A sample placed in a reactor will be exposed to varying neutron fluence, Φ, dependent on location from the neutron source. The space-average fluence, Φ, is the time-integrated space-averaged flux, defined as

$$\Phi = \int \phi(t)dt\,, \tag{1}$$

with the space-averaged total neutron flux defined as

$$\phi(t) = \frac{\iint \phi(\boldsymbol{r}, E, t)dEd\boldsymbol{r}}{\int d\boldsymbol{r}}. \tag{2}$$

Reacting material is assumed to be exposed to the same neutron fluence. Fluence is a time-integrated variable and is the integration factor adjusted during the evaluation process. Destruction of isotopes occur by the (n,f), (n,γ), (n,2n) and (n,3n) reactions. Subsequently production is due to the (n,γ), (n,2n) and (n,3n) reactions. A simple rate equation transformed from time dependency to fluence dependency is

$$\frac{dN_x(X_z)}{dX_z} = \sum_{i=\gamma,2n,3n} \frac{\langle \sigma_i^y \rangle}{\langle \sigma_f^z \rangle} N_y(X_z) - \sum_{j=\gamma,2n,3n,f} \frac{\langle \sigma_j^x \rangle}{\langle \sigma_f^z \rangle} N_x(X_z). \quad (3)$$

Where $y \neq x$ with the destruction of nuclide N_x by all reactions and creation by the neutron reactions $N_{y=x-1}$(n,γ)N_x, $N_{y=x+1}$(n,2n) N_x and $N_{y=x+2}$ (n,3n) N_x. A "fission conversion fraction", X_z, is defined by

$$X_z = \langle \sigma_f^z \rangle \Phi \Rightarrow dX_z = \langle \sigma_f^z \rangle d\Phi, \quad (4)$$

where $\langle \sigma_f^z \rangle$ is the average fission cross section for the reference nuclide *z*. The reference nuclide is dependent on the source of the neutrons.

Neutron flux-weighted average reaction cross sections are defined by

$$\langle \sigma_i^y \rangle = \frac{\int \phi(\boldsymbol{r}, E, t) \sigma_i^y(E) dE}{\int \phi(\boldsymbol{r}, E, t) dE} = \frac{\int \phi(\boldsymbol{r}, E, t) \sigma_i^y(E) dE}{\phi(\boldsymbol{r}, t)}, \quad (5)$$

and

$$\langle \sigma_j^x \rangle = \frac{\int \phi(\boldsymbol{r}, E, t) \sigma_j^x(E) dE}{\int \phi(\boldsymbol{r}, E, t) dE} = \frac{\int \phi(\boldsymbol{r}, E, t) \sigma_j^x(E) dE}{\phi(\boldsymbol{r}, t)}. \quad (6)$$

Where:

$\phi(\boldsymbol{r}, E, t)$	=	neutron flux
$\phi(\boldsymbol{r}, t)$	=	total neutron flux
$\boldsymbol{r}$	=	space vector
E	=	energy
t	=	time

— 3 — Cross Section Measurements

Cross section measurements at LANL initially were carried out in critical assemblies from the 1950's to the 1970's. Each assembly maintained a unique neutron spectrum that varied on location within the assembly. Different fissionable materials arranged in various geometries were used to construct the assemblies. Actinide and detector cross section experiments were performed. After bombardment, samples are analyzed for activity of fission products and products of other neutron reactions of interest for the particular experiment. Number of fissions that took place in fissionable material in the foil can be deduced by measuring the activity of ^{99}Mo or ^{147}Nd. The critical assemblies experiments used for the development of the IPC cross section library are listed in Table 3-1 along with the sample materials investigated. Archival photographs of the Flattop, JEZEBEL, Godiva and BIG-10 assemblies are displayed in Figure 3-1.

Table 3-1 Critical Assemblies and Sample Material Experimented through 1967 to 1970. [1]

Critical Assembly	Sample Material
Oralloy Core Tuballoy Tamper FLATTOP	Oy, Pu+Am, D-38 (depleted uranium), $^{236}U_3O_8$, K_3IrCl_6, $IrCl_3$, Zr, Th, Pt, Nb, Ag, Tm, Lu, ^{203}Tl, Au, Er, Ho, NaF, S, W, Ta, Bi, As, Sc_2O_3,V
Plutonium Core Tuballoy Tamper FLATTOP	Oy, Pu+Am, D-38, ^{238}U, Au, Th, Ag, Tm, Lu, Tl, $K_2{}^{193}IrCl_6$, K_2IrCl_6
Plutonium JEZEBEL	Oy, Pu(low Am), Pu(high Am), D-38, K_2IrCl_6, Tm
BIG 10	^{235}U, ^{238}U, ^{237}Np,^{239}Pu
GODIVA	^{235}U, ^{238}U, ^{233}U,^{239}Pu,D-38, Th

The Godiva assembly is a bare sphere of enriched uranium that began operation in 1951. The sphere is split into three sections, a stationary central section with retractable lower and upper caps. This assembly became a radiation source which produced approximately 1000 prompt-radiation bursts. In 1957 an incident caused serve warping and oxidation of parts and damage to the supports, the assembly has to be retired and replaced by Godiva II. [2]

Jezebel is a non-reflected spherical assembly of delta-phase plutonium containing 4.5% ^{240}Pu that became operational in 1954. As with the Godiva assembly, Jezebel was split into a central section and two end caps. Two different components were mounted temporarily on the Jezebel machine during the 1960's. The first was uranium metal containing 98.1% ^{233}U and the second was delta-phase plutonium containing 20.1% ^{240}Pu. Afterwards Jezebel was operated with the original 4.5% ^{240}Pu spectrum through May 1977. [2]

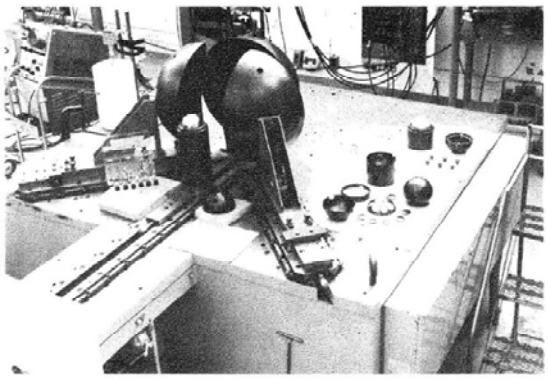

(a)

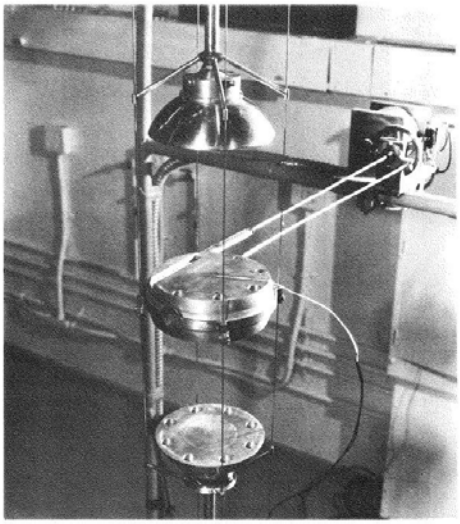

Fig. 16.
The Jezebel assembly of unreflected plutonium. For operation, the upper cap drops and the lower cap rises to form a near-sphere.

(b)

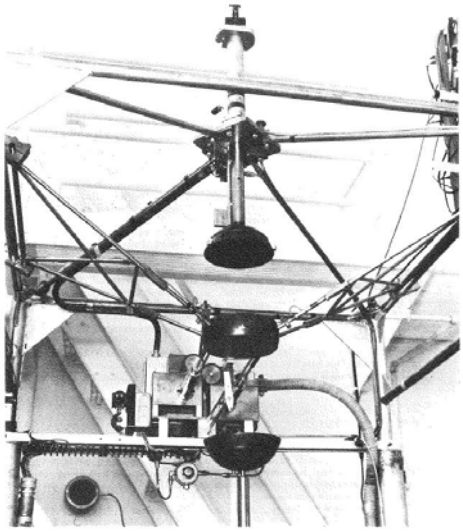

Fig. 13.
The Lady Godiva critical assembly of highly enriched uranium. For operation, the upper cap drops and the lower cap rises to form a near-sphere without reflector.

(c)

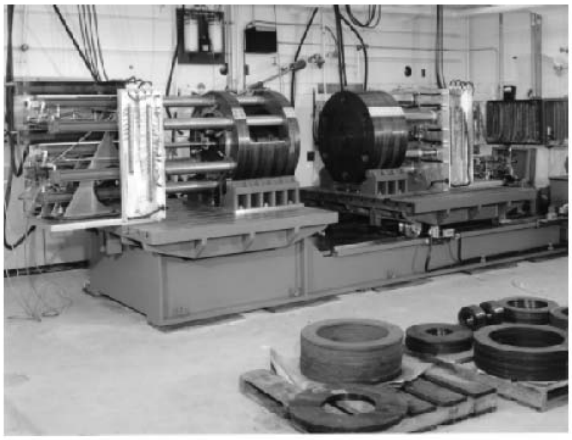

Figure 1 The Big Ten Assembly during Construction (1968)

(d)

Figure 3-1 (a) Flattop (b) JEZEBEL, (c) Godiva and (d) BIG 10 Assemblies [2]

The Flattop assembly is consists of a massive bed which supports a natural uranium sphere which one hemisphere is stationary. Two quadrants of the moveable hemisphere travel on tracks. Buttons of core material can replace natural uranium adapters in the sphere. Cores of orally, ^{239}Pu and ^{233}U are used. Transverse measurements at various locations from center are possible with this assembly. [2]

Big-10 is an all uranium assembly with a low ^{235}U enriched core. It consists of a 21-inch diameter cylindrical core surrounded by a 6-inch thick uranium reflector. The core length was adjustable controlling excess reactivity. [2]

3.1 Cross Section Computations

Cross sections for neutron induced reactions in a material exposed to a neutron flux for a defined period of time can be defined in terms of the number of atoms produced from the reaction, N_P, and atoms in the target, N_T as [3]

$$\sigma = \frac{N_P}{N_T} \cdot \frac{1}{\Phi}. \tag{7}$$

Experiments are performed with a reference reaction so the spaced-averaged fluence,Φ, can be defined as

$$\Phi = \frac{N_P^r}{N_T^r} \cdot \frac{1}{\sigma^r}. \tag{8}$$

Rearranging and substituting gives the following cross section for the sample material in terms of the reference material,

$$\frac{\sigma}{\sigma^r} = \frac{N_P}{N_T} \cdot \frac{N_T^r}{N_P^r}. \tag{9}$$

Measuring relative cross sections instead of absolute measurements eliminates the need for knowledge of the neutron flux at the location of irradiation. Solution to the fluence-based rate equations used in IPC requires knowledge of the relative averaged cross sections as a function of the harness of the neutron spectrum. An initial hardness of the neutron spectrum is established for each sample being evaluated. The hardness of the fission neutron spectrum is not measured directly but is calibrated in terms of a "spectral index".

3.2 Fission Spectrum Regime Spectral Index

Historically the "uranium-fission ratio", $\sigma_f^{238}/\sigma_f^{235}$, defined as ratio of the (n,f) reaction cross sections for ^{238}U and ^{235}U respectively was defined to serve as this index. The ^{238}U fission cross section drops significantly below 2 MeV and thresholds at approximately 0.5 MeV with the ^{235}U fission cross section remaining nearly constant over fission spectrum energies. This is shown graphically in Figure 3-2. Therefore a decrease in the ratio corresponds to a softening neutron spectrum. Packets containing elemental and uranium foils are placed at various locations in the

assembly to measure reaction cross sections as a function of neutron energy for a specific spectral hardness as indicated by the "uranium fission ratio". Work performed in the 1960's indicated that two iridium isotopes might also serve as a "spectral index".

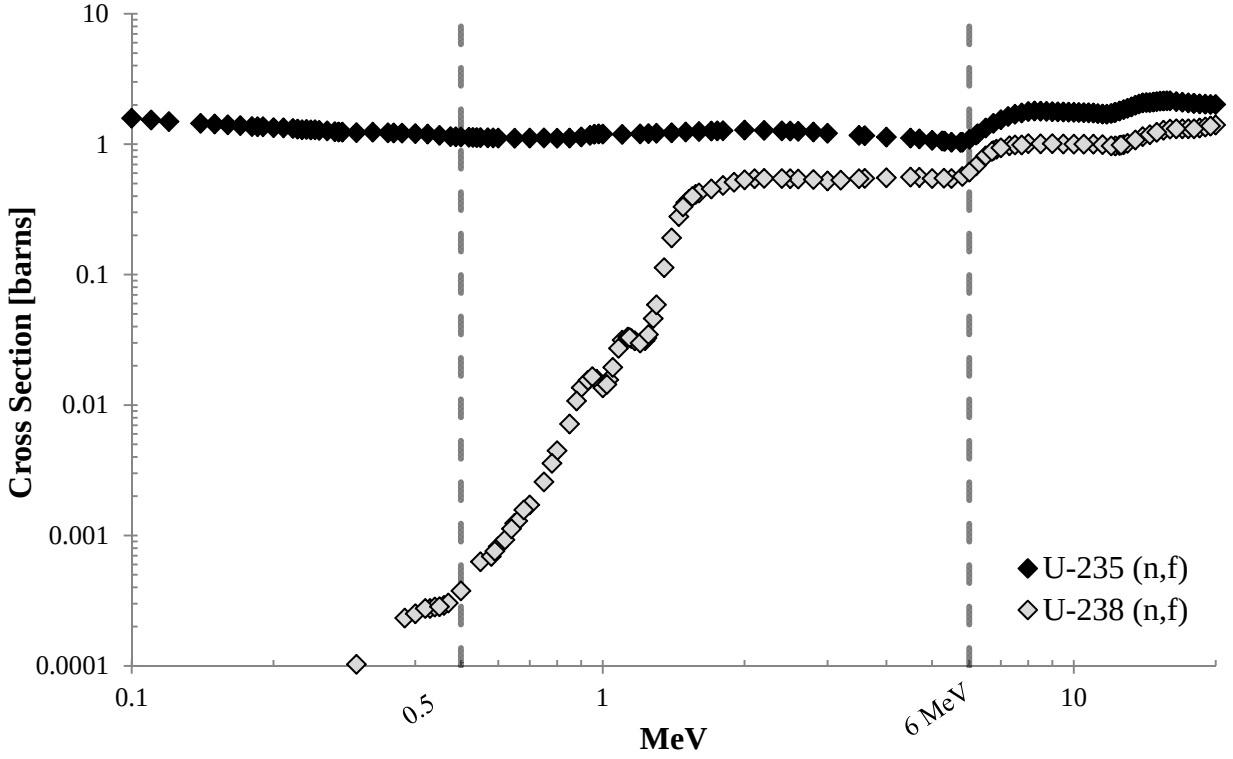

Figure 3-2 ENDF/B-VII.I evaluated neutron fission reaction data for ^{235}U and ^{238}U.

Natural iridium has only two stable isotopes, ^{191}Ir and ^{193}Ir. The heavier isotope has a metastable nuclear state, ^{193m}Ir, that is populated through the inelastic neutron scattering reaction ^{193}Ir(n, n')^{193m}Ir. This scattering cross section has substantial amplitude over the range of fission spectrum neutron energies with a threshold of about 80 keV. Neutron capture reaction on ^{191}Ir produces the ^{192}Ir isotope, ^{191}Ir(n, γ)^{192}Ir. The ^{192}Ir isotope is also populated through the (n, 2n) reaction on ^{193}Ir. Up to neutron energies of 6 MeV, the production of ^{192}Ir is dominated by the (n, γ) reaction. In addition the (n,2n) reaction on ^{191}Ir will produce ^{190}Ir. The ratio of ^{193m}Ir/^{192}Ir decreases monotonically as the hardness of the spectrum decreases making it a suitable choice for the "spectral index". This relationship is shown in Figure 3-3.

The iridium spectral ratio is referred to as the "Ratio Iridium" or RIR. The ratio is defined as

$$RIR = \frac{N_{193m}}{N_{192}}. \tag{10}$$

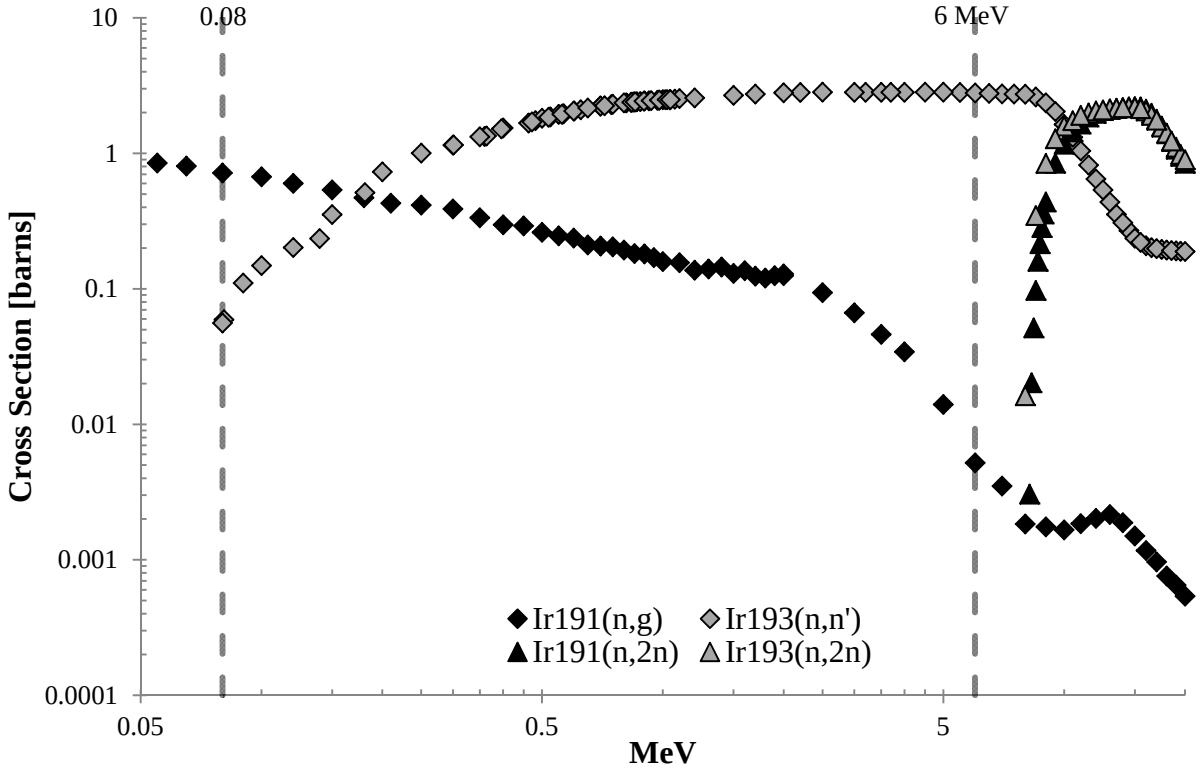

Figure 3-3 ENDF/B-VII.I evaluated neutron fission reaction data for ^{191}Ir and ^{193}Ir.

3.3 Iridium Cross Section Measurements

Iridium foil packets are placed in critical assemblies and are activated by the following neutron reactions:

$$^{191}\text{Ir}(n,\gamma)^{192}\text{Ir}$$

$$^{191}\text{Ir}(n,2n)^{190}\text{Ir}$$

$$^{193}\text{Ir}(n,n')^{193m}\text{Ir}$$

$$^{193}\text{Ir}(n,2n)^{192}\text{Ir}$$

Activity of the iridium isotopes, ^{190}Ir, ^{192}Ir and ^{193m}Ir, are measured after irradiation. Atom ratios from the inelastic neutron scattering reaction on ^{193}Ir and the (n,2n) reaction on ^{191}Ir is straight forward to calculate due to a lack of a competing reaction. Atom ratios are calculated by

$$\frac{N_{193(n,n')193m}}{N_{193^o}} = \frac{(CPM \times K/\gamma_{193m})_{193m_{Ir}}}{(N_A/W_{Ir}) \times \theta_{193_{Ir}}} \tag{11}$$

and

$$\frac{N_{191(n,2n)190}}{N_{191^o}} = \frac{(CPM \times K/\gamma_{190})_{190_{Ir}}}{(N_A/W_{Ir}) \times \theta_{191_{Ir}}}. \quad (12)$$

Where

γ	=	Irradiation Correction Factor
K	=	Conversion factor from CPM to atoms
CPM	=	Counts per minute
N_A	=	Avogadro's number
W	=	Atomic weight
θ	=	Isotopic abundance

Determination of the number of ^{192}Ir atoms from the (n,γ) reaction on ^{191}Ir is complicated by the fact the ^{192}Ir is produced from a competing reaction, the (n,2n) reaction on ^{193}Ir. The measured atoms of ^{192}Ir are due to both reactions and cannot be distinguished from each other. A correction must be applied to determine the cross section for the (n,γ) reaction alone.

$$\frac{N_{191(n,\gamma)192}}{N_{191^o}} = \frac{N_{192}}{N_{191^o}} - \frac{N_{191(n,2n)190}}{N_{191^o}} \times C \quad (13)$$

Where C is a correction factor defined as

$$C = \frac{N_{193^o}}{N_{191^o}} \times \frac{\sigma^{14}_{193Ir(n,2n)^{192}Ir}}{\sigma^{14}_{191Ir(n,2n)^{190}Ir}} = \frac{N_{193(n,2n)192}}{N_{191(n,2n)190}}. \quad (14)$$

Historically the correction factor was determined to be 1.73. Using current ENDF/B-VII.I interpreted data this factor is estimated to be 1.68. A correction of 1.41% is required when the historical factor is used compared to 1.37% using ENDF/B-VII.I. Both factors results in a similar correction to the measured ^{192}Ir data. Correction factor based on ENDF/B-VII.I data is applied for the results presented in this document.

The iridium spectral index is calculated by

$$\frac{N_{193(n,n')193m}}{N_{191(n,\gamma)192}} = \frac{\sigma^{fs}_{193_{Ir}(n,n')193m_{Ir}}}{\sigma^{fs}_{191_{Ir}(n,\gamma)192_{Ir}}} \cdot \frac{N_{193^o}}{N_{191^o}}. \quad (15)$$

— 4 — Actinide Cross Section Measurements

Actinide isotopes activated in the critical assemblies are ^{239}Pu, ^{235}U and ^{238}U. Foils of these reference materials were placed in the same location as the iridium foils. The reaction is neutron

induced fission. The fission cross section is simply defined as the ratio of the number of fissions that occurred, *F*, and the initial number of atoms of the reference material divided by the neutron fluence as follows:

$$\sigma_{(n,f)}^{^{239}Pu} = \frac{F_{^{239}Pu}}{N^{o}_{^{239}Pu}} \cdot \frac{1}{\Phi} \tag{16}$$

$$\sigma_{(n,f)}^{^{235}U} = \frac{F_{^{235}U}}{N^{o}_{^{235}U}} \cdot \frac{1}{\Phi} \tag{17}$$

$$\sigma_{(n,f)}^{^{238}U} = \frac{F_{^{238}U}}{N^{o}_{^{238}U}} \cdot \frac{1}{\Phi} \tag{18}$$

The initial number of atoms is calculated by

$$N^{o}_{^{239}Pu} = mass \times \omega_{Pu} \times \omega_{^{239}Pu} \times \frac{N_A}{W_{^{239}Pu}}, \tag{19}$$

$$N^{o}_{^{235}U} = mass \times \omega_{U} \times \omega_{^{235}U} \times \frac{N_A}{W_{^{235}U}}, \tag{20}$$

and

$$N^{o}_{^{238}U} = mass \times \omega_{U} \times \omega_{^{238}U} \times \frac{N_A}{W_{^{238}U}}. \tag{21}$$

Where ω is the weight percent which is defined in terms of the atom ratios, *N*, and atomic weight ratios, *W*, as

$$\omega_{^{239}Pu} = \frac{1}{1+\frac{W_{^{239}Pu}}{W_{^{240}Pu}}\frac{N_{^{240}Pu}}{N_{^{239}Pu}}+\frac{W_{^{239}Pu}}{W_{^{241}Pu}}\frac{N_{^{241}Pu}}{N_{^{239}Pu}}+\frac{W_{^{239}Pu}}{W_{^{242}Pu}}\frac{N_{^{242}Pu}}{N_{^{239}Pu}}}, \tag{22}$$

$$\omega_{^{235}U} = \frac{1}{1+\frac{W_{^{235}U}}{W_{^{234}U}}\frac{N_{^{234}U}}{N_{^{235}U}}+\frac{W_{^{235}U}}{W_{^{236}U}}\frac{N_{^{236}U}}{N_{^{235}U}}+\frac{W_{^{235}U}}{W_{^{238}U}}\frac{N_{^{238}U}}{N_{^{235}U}}}, \tag{23}$$

and

$$\omega_{^{238}U} = \frac{1}{1+\frac{W_{^{238}U}}{W_{^{235}U}}\frac{N_{^{235}U}}{N_{^{238}U}}}. \tag{24}$$

Atom ratios are determined from mass spectrometry measurements. Fissions in plutonium for experiments with and without significant amounts of americium are defined by

$$F_{Pu} = \Phi\left\{N_{239_{Pu}}\sigma_{239_{Pu}} + N_{240_{Pu}}\sigma_{240_{Pu}} + N_{241_{Pu}}\sigma_{241_{Pu}} + N_{242_{Pu}}\sigma_{242_{Pu}}\right\} = \Phi N_{239_{Pu}}\sigma_{239_{Pu}}\left\{1 + \frac{N_{240_{Pu}}}{N_{239_{Pu}}}\frac{\sigma_{240_{Pu}}}{\sigma_{239_{Pu}}} + \frac{N_{241_{Pu}}}{N_{239_{Pu}}}\frac{\sigma_{241_{Pu}}}{\sigma_{239_{Pu}}} + \frac{N_{242_{Pu}}}{N_{239_{Pu}}}\frac{\sigma_{242_{Pu}}}{\sigma_{239_{Pu}}}\right\} = F_{239_{Pu}}\,\Omega_{239_{Pu}}, \quad (25)$$

and

$$F_{Pu} = \Phi\left\{N_{239_{Pu}}\sigma_{239_{Pu}} + N_{240_{Pu}}\sigma_{240_{Pu}} + N_{241_{Pu}}\sigma_{241_{Pu}} + N_{242_{Pu}}\sigma_{242_{Pu}} + N_{241_{Am}}\sigma_{241_{Am}}\right\} = \Phi N_{239_{Pu}}\sigma_{239_{Pu}}\left\{1 + \frac{N_{240_{Pu}}}{N_{239_{Pu}}}\frac{\sigma_{240_{Pu}}}{\sigma_{239_{Pu}}} + \frac{N_{241_{Pu}}}{N_{239_{Pu}}}\frac{\sigma_{241_{Pu}}}{\sigma_{239_{Pu}}} + \frac{N_{242_{Pu}}}{N_{239_{Pu}}}\frac{\sigma_{242_{Pu}}}{\sigma_{239_{Pu}}} + \frac{N_{241_{Am}}}{N_{239_{Pu}}}\frac{\sigma_{241_{Am}}}{\sigma_{239_{Pu}}}\right\} = F_{239_{Pu}}\,\Omega_{239_{Pu}}. \quad (26)$$

Fissions in uranium foils are defined by

$$F_{Oy} = \Phi\left\{N_{234_U}\sigma_{234_U} + N_{235_U}\sigma_{235_U} + N_{236_U}\sigma_{236_U} + N_{238_U}\sigma_{238_U}\right\} = \Phi N_{235_U}\sigma_{235_U}\left\{1 + \frac{N_{234_U}}{N_{235_U}}\frac{\sigma_{234_U}}{\sigma_{235_U}} + \frac{N_{236_U}}{N_{235_U}}\frac{\sigma_{236_U}}{\sigma_{235_U}} + \frac{N_{238_U}}{N_{235_U}}\frac{\sigma_{238_U}}{\sigma_{235_U}}\right\} = F_{235_U}\,\Omega_{235_U}, \quad (27)$$

and

$$F_{DU} = \Phi\left\{N_{234_U}\sigma_{234_U} + N_{235_U}\sigma_{235_U} + N_{236_U}\sigma_{236_U} + N_{238_U}\sigma_{238_U}\right\} = \Phi N_{238_U}\sigma_{238_U}\left\{1 + \frac{N_{235_U}}{N_{238_U}}\frac{\sigma_{235_U}}{\sigma_{238_U}}\right\} = F_{238_U}\,\Omega_{238_U}. \quad (28)$$

Fission cross sections can then be determined by rearrangement of the above equations:

$$\sigma_{(n,f)}^{239_{Pu}} = \frac{F_{239_{Pu}}}{N^o_{239_{Pu}}}\cdot\frac{1}{\Phi} = \frac{F_{Pu}}{N^o_{239_{Pu}}}\cdot\frac{1}{\Omega_{239_{Pu}}}\cdot\frac{1}{\Phi} \quad (29)$$

$$\sigma_{(n,f)}^{235_U} = \frac{F_{235_U}}{N^o_{235_U}}\cdot\frac{1}{\Phi} = \frac{F_{Oy}}{N^o_{235_U}}\cdot\frac{1}{\Omega_{235_U}}\cdot\frac{1}{\Phi} \quad (30)$$

$$\sigma_{(n,f)}^{238_U} = \frac{F_{238_U}}{N^o_{238_U}}\cdot\frac{1}{\Phi} = \frac{F_{DU}}{N^o_{238_U}}\cdot\frac{1}{\Omega_{238_U}}\cdot\frac{1}{\Phi} \quad (31)$$

Fissions in the plutonium, oralloy and depleted uranium foils are obtained from the fission product ^{99}Mo measurements:

$$F_{Pu} = \frac{CPM_{^{99}Mo}}{\gamma} K_{^{99}Mo}^{fs.^{239}Pu} \quad (32)$$

$$F_{Oy} = \frac{CPM_{^{99}Mo}}{\gamma} K_{^{99}Mo}^{fs.^{235}U} \quad (33)$$

$$F_{DU} = \frac{CPM_{^{99}Mo}}{\gamma} K_{^{99}Mo}^{fs.^{238}DU} \quad (34)$$

An irradiation correction, γ, is applied to the measured counts, CPM. These are taken as reported in the Pajarito Irradiation Notebook [1].

4.1 Determination of the Fission Factor

A fission factor, Ω, is defined as a function of the atom ratios of the foil material and the expected fission cross section ratios of the critical assembly. Table 4-1 lists the fissions factors calculated using fission cross section ratios and mass spectrometry results reported in the Pajarito Irradiations Notebook [1] for core assembly measurements. Historic cross section ratios reported for the plutonium core Flattop assembly experiment in 1967 are given in Table 4-2.

Fission cross section ratios were reevaluated in fission counting experiments in an all uranium critical assembly at Los Alamos in 1971. Data from these experiments can be found in a radiochemistry notebook by D.W. Barr [4] on pages 72 to 82. Discs of ^{235}U, ^{236}U, ^{238}U, ^{239}Pu, ^{240}Pu, ^{241}Pu, ^{242}Pu and ^{241}Am irradiated in a dual fission chamber. Using the reported data a solver programmed in MATLAB is used to determine the cross section ratios. These results are given in Table 4-3. Based on these cross section ratios, fissions factors are calculated using mass spectrometry reports from 1970 and listed in Table 4-4. A measurement for ^{234}U was not performed in the 1971experiments so the value reported for a plutonium core was assumed. The reevaluated results compared to that reported in the Pajarito notebook for the Flattop assembly with a uranium core.

As reported fission cross section ratios for the Jezebel and Big-10 assemblies are given in Table 4-5 and Table 4-6. There is a discrepancy between 1974 and 1976 uranium fission cross section ratios for the Big-10 experiments. For the results presented in this work the associated year the ratios were reported are used. When the 1976 fission factor is used with the 1974 data, a difference of 0.17% between the calculated fissions is observed, which is deemed to be insignificant.

Measurements in the Flattop assembly can be performed at center as well at varying locations from the core. Accordingly the fission cross section ratios becomes a function of the distance from the core. The first Flattop traverse experiment was conducted on August 18, 1970 and

involved activating foils of oralloy, depleted uranium and iridium. Uranium fission factors as function of position in the assembly for this experiment are reported in Table 4-7. These factors were not explicitly reported so they had to be assessed from reported fission data. A second experiment was run in April 19, 1971 with plutonium, oralloy and ^{236}U foils. The fission factors were reported in the Pajarito notebook and are provide in Table 4-8. A graphical comparison between the uranium fission factors in given in Figure 4-1. The diminution of the hardness of the neutron spectrum for the experiment is evident.

Overall the fission factors are comparable between the two experiments. A polynomial fit was applied to the ^{235}U fission factor data from the 1971 experiment. The resulting function was used to calculate the fission factors for the 1970 experiment to investigate the possible discrepancies. These results along with the relative difference are reported in Table 4-9. The difference is insignificant so the ^{235}U fission factor as determined from the reported data from the 1970 experiment is used for the work presented in this document.

Table 4-1 Cross section factors used for Pajarito experiments used to determine fission in the reference material. Calculated using data reported in the Pajarito Irradiations Notebook. [1]

	Date of Irradiation	$\boldsymbol{\Omega_{239_{Pu}}}$	$\boldsymbol{\Omega_{235_{U}}}$	$\boldsymbol{\Omega_{238_{U}}}$
Plutonium Core Flattop (Center)	8/10/1967	1.034	1.019	-
Oralloy Core Flattop (Center)	4/29/1968	1.033	0.018	-
Oralloy Core Flattop (Center)	4/7/1969	-	0.018	-
Plutonium Core Flattop (Center)	8/5/1970	1.034*	-	1.004
Plutonium Jezebel (Center)	10/23/1973	1.039	1.023	1.004
Big-10 (Center)	7/9/1974	-	1.0049	1.00032
Big-10 (Center)	1/27/1976	1.024	1.0066	-

* Corrected using revaluated fission cross section ratios and mass spectrometry report from 1970. Pajarito notebook [1] reported 1.033.

Table 4-2 Fission cross section ratios reported in the Pajarito Irradiations Notebook [1] for Flattop with a plutonium core.

$\frac{\sigma_{240_{Pu}}}{\sigma_{239_{Pu}}}$	0.57	$\frac{\sigma_{234_{U}}}{\sigma_{238_{U}}}$	0.74
$\frac{\sigma_{241_{Pu}}}{\sigma_{239_{Pu}}}$	0.98	$\frac{\sigma_{236_{U}}}{\sigma_{235_{U}}}$	0.32
$\frac{\sigma_{242_{Pu}}}{\sigma_{239_{Pu}}}$	0.49	$\frac{\sigma_{238_{U}}}{\sigma_{235_{U}}}$	0.16

Table 4-3 Evaluated fission cross section ratios for fission counting experiments performed in 1971 in all uranium critical assembly.

$\frac{\sigma_{238_{Pu}}}{\sigma_{239_{Pu}}}$	1.004	$\frac{\sigma_{236_U}}{\sigma_{235_U}}$	0.316
$\frac{\sigma_{240_{Pu}}}{\sigma_{239_{Pu}}}$	0.549	$\frac{\sigma_{238_U}}{\sigma_{235_U}}$	0.140
$\frac{\sigma_{241_{Pu}}}{\sigma_{239_{Pu}}}$	1.076	$\frac{\sigma_{239_{Pu}}}{\sigma_{235_U}}$	1.307
$\frac{\sigma_{242_{Pu}}}{\sigma_{239_{Pu}}}$	0.483	$\frac{\sigma_{241_{Am}}}{\sigma_{239_{Pu}}}$	0.576

Table 4-4 Calculated fission factors using revaluated fission cross section from the fission counting experiments performed in 1971. Atom ratios were taken from mass spectrometry reports given in the Pajarito Irradiation Notebook [1] from 1970. The value of 0.74 was assumed for $^{234}U/^{235}U$ since a measurement was not made in the 1971 experiment.

$\Omega_{239_{Pu}}$	Ω_{235_U}	Ω_{238_U}
1.034	1.018	1.005

Table 4-5 Fission cross section ratios reported in the Pajarito Irradiations Notebook [1] for the Jezebel critical assembly.

$\frac{\sigma_{240_{Pu}}}{\sigma_{239_{Pu}}}$	0.600	$\frac{\sigma_{234_U}}{\sigma_{238_U}}$	0.85
$\frac{\sigma_{241_{Pu}}}{\sigma_{239_{Pu}}}$	1.020	$\frac{\sigma_{236_U}}{\sigma_{235_U}}$	0.400
$\frac{\sigma_{242_{Pu}}}{\sigma_{239_{Pu}}}$	0.540	$\frac{\sigma_{238_U}}{\sigma_{235_U}}$	0.200

Table 4-6 Fission cross section ratios reported in the Pajarito Irradiations Notebook [1] for the Big-10 experiments performed in 1974 and 1976.

Big-10 9/19/1974		**Big-10 1/27/1976**			
$\frac{\sigma_{234_U}}{\sigma_{238_U}}$	0.310	$\frac{\sigma_{234_U}}{\sigma_{238_U}}$	0.34	$\frac{\sigma_{240_{Pu}}}{\sigma_{239_{Pu}}}$	0.319
$\frac{\sigma_{236_U}}{\sigma_{235_U}}$	0.110	$\frac{\sigma_{236_U}}{\sigma_{235_U}}$	0.128	$\frac{\sigma_{241_{Pu}}}{\sigma_{239_{Pu}}}$	1.21
$\frac{\sigma_{238_U}}{\sigma_{235_U}}$	0.0374	$\frac{\sigma_{238_U}}{\sigma_{235_U}}$	0.0372	$\frac{\sigma_{242_{Pu}}}{\sigma_{239_{Pu}}}$	0.253
				$\frac{\sigma_{241_{Am}}}{\sigma_{239_{Pu}}}$	0.252

Table 4-7 Fission factor variability across the oralloy Flattop traverse conducted on 08/18/1970. These factors were not reported directly in the Pajarito notebook [4] and required a solver to determine.

Distance from Center [cm]	Ω_{235_U}	Ω_{238_U}
1.11	1.0180	1.0050
0.875	1.0181	1.0050
3.54	1.0177	1.0034
5.05	1.0166	1.0044
5.72	1.0148	1.0052
8.2	1.0086	1.0104
10.82	1.0064	1.0169
14.63	1.0039	1.0278

Table 4-8 Fission factor variability across the oralloy Flattop traverse conducted on 4/19/1971. These are as reported in the Pajarito notebook on page 27 [1].

Distance from Center [cm]	$\Omega_{239_{Pu}}$	**Distance from Center [cm]**	Ω_{235_U}	**Distance from Center [cm]**	Ω_{236_U}
0.60	1.0375	0.2	1.0175	0.2	1.0062
1.2	1.0374	0.8	1.0175	1.1	1.0062
4.1	1.0362	5.0	1.0154	5.0	1.0070
5.1	1.0348	1.0	1.0175	1.0	1.0062
4.80	1.0353	3.9	1.0165	3.7	1.0066
8.3	1.0250	4.9	1.0156	5.8	1.0069
11.2	1.0209	8.1	1.0083	8.4	1.0128
15.5	1.0177	11.0	1.0058	11.0	1.0193
		15.3	1.0041	14.8	1.0290

Table 4-9 Comparison of two methods to determine the ^{235}U fission factors for the Flattop traverse experiment in 1970. The first method used the as reported data in the Pajarito Irradiation Notebook [1]. Using the polynomial fit obtained from the 1971 reported fission factors, the fission factors for the 1970 experiment were recalculated.

Radius [cm]	Based on 1970 Data Ω_{235_U}	Based on fit of 1971 Data Ω_{235_U}	%Difference
1.11	1.0180	1.0178	0.03%
0.875	1.0181	1.0177	0.04%
3.54	1.0177	1.0168	0.09%
5.05	1.0166	1.0149	0.17%
5.72	1.0148	1.0138	0.10%
8.2	1.0086	1.0094	0.08%
10.82	1.0064	1.0052	0.13%
14.63	1.0039	1.0035	0.04%

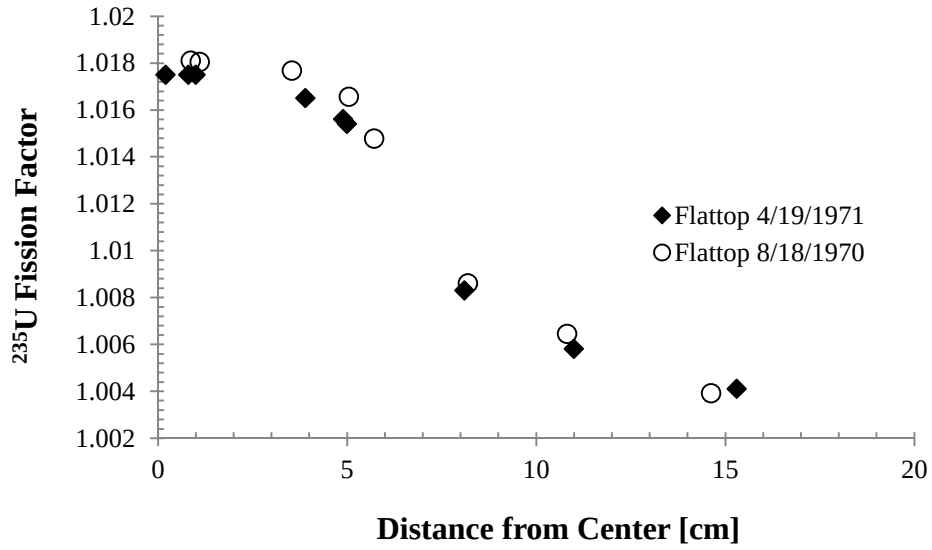

Figure 4-1 Comparison of ^{235}U fission factors for the two Flattop experiments performed with an oralloy core.

4.2 Establishing K-factors

Foils are counted for several fission products including ^{99}Mo and ^{147}Nd. K-factors are used to convert counts to fissions. They are detector dependent therefore have been variable over the course of the critical assembly experiments performed at LANL. Summarized in Table 4-10 and Table 4-11 are the K-factors and ^{147}Nd R-values adopted for this body of work.

Uncertainty was propagated for the K-factors based on the statistical uncertainty quoted on the ^{235}U thermal ^{99}Mo K-factor and uncertainty reported by Selby et al. for Q-values [5]. The significant component of uncertainty in the calculation of the fissions based on ^{99}Mo measurements will be the associated K-factors. K-factors for ^{147}Nd are relative to ^{99}Mo k-factors using associated r-values and R-values, therefore the uncertainty will be higher. For this reason, fission based on ^{99}Mo will only be used for this work, not an average between ^{99}Mo and ^{147}Nd as was historically done.

Table 4-10 Adopted ^{99}Mo K-factors for Counter 6.

	Prior to 1970	**1970 to Present**
$K_{99_{Mo}}^{235_{U},th}$	2.333E+05 ± 0.8%**	2.459E+05 ± 0.85%
$K_{99_{Mo}}^{239_{Pu},th}$	2.286E+05 ± 2.62%	2.410E+05 ± 2.64%
$K_{99_{Mo}}^{235_{U},fs}$	2.334E+05 ± 2.06%	2.460E+05 ± 2.08%
$K_{99_{Mo}}^{239_{Pu}fs}$	2.299E+05 ± 2.15%	2.423E+05 ± 2.17%
$K_{99_{Mo}}^{238_{U},fs}$	2.277E+05 ± 2.34%	2.400E+05 ± 2.36%
$K_{99_{Mo}}^{235_{U},f}$	2.710E+05 ± 3.3%	2.856E+05 ± 3.31%
$K_{99_{Mo}}^{239_{Pu}f}$	2.506E+05 ± 3.4%	2.641E+05 ± 3.41%
$K_{99_{Mo}}^{238_{U},f}$	2.440E+05 ± 3.4%	2.572E+05 ± 3.41%

Table 4-11 Adopted ^{147}Nd K-factors.

	Prior to 1970 Counter 6	**1970 to Present Counter 6**	**1970 to Present Counter 13**
$K_{99_{Mo}}^{235_{U},th}$	7.616E+06 ± 1.55%	8.074E+06 ± 0.86%	7.789E+06 ± 1.14%
$K_{99_{Mo}}^{239_{Pu},th}$	8.424E+06 ± 4.60%	8.931E+06 ± 4.41%	8.616E+06 ± 4.48%
	Selby et al. R-Values	Selby et al. R-Values	Selby et al. R-Values
$K_{99_{Mo}}^{235_{U},fs}$	7.806E+06 ± 2.5%	8.276E+06 ± 2.14%	7.984E+06 ± 2.27%
$K_{99_{Mo}}^{239_{Pu}fs}$	8.192E+06 ± 2.66%	8.684E+06 ± 2.32%	8.378E+06 ± 2.44%
$K_{99_{Mo}}^{238_{U},fs}$	6.396E+06 ± 2.76%	6.780E+06 ± 2.44%	6.541E+06 ± 2.55%
	Mac Innes et al R-Values	Mac Innes et al R-Values	Mac Innes et al R-Values
$K_{99_{Mo}}^{235_{U},f}$	9.983E+06 ± 4.18%	1.047E+07 ± 3.98%	1.010E+07 ± 4.05%
$K_{99_{Mo}}^{239_{Pu}f}$	8.969E+06 ± 4.85%	8.946E+06 ± 4.68%	8.631E+06 ± 4.74%
$K_{99_{Mo}}^{238_{U},f}$	7.887E+06 ± 3.91%	8.170E+06 ± 3.69%	7.882E+06 ± 3.76%
rth	0.03063 ± 1.3%	0.03046 ± 0.3%	0.03157 ± 0.75% [6]

— 5 — Reevaluation of Pajarito Experiments

Data from the Flattop, Jezebel and Big-10 critical assembly experiments from 1968 to 1976 are reassessed. Fissions per sample are determined from the fission product ^{99}Mo rather than an average between ^{147}Nd and ^{99}Mo. Measurements performed on the traverse of Flattop assembly with an oralloy core did not include ^{147}Nd, so an average cannot be taken. In order to maintain conformability between the experiments, only the ^{99}Mo measurements are used from those experiments that included measurements for ^{147}Nd and ^{99}Mo. In addition the K-factor for ^{147}Nd is dependent on the ^{99}Mo K-factor, so uncertainty is larger when the average is utilized. Calculated fissions and the associated uncertainty are given in Table 5-1 for ^{235}U samples comparing the difference between using only ^{99}Mo fissions and an average of ^{99}Mo and ^{147}Nd fissions.

Table 5-1 Comparison of calculated fissions in ^{235}U samples using an average between ^{99}Mo and ^{147}Nd and ^{99}Mo only. Modern K-factors are used to convert counts to fissions. Uncertainty has been propagated and includes error on counts measured and K-factor.

	Date of Irradiation	Fissions (^{99}Mo and ^{147}Nd)	Fissions (^{99}Mo)
Oralloy Core Flattop (Center)	4/7/1969	3.032E+11 ± 3.0%	3.081E+11 ± 2.3%
Plutonium Core Flattop (Center)	8/5/1970	7.332E+11 ± 3.6%	7.390E+11 ± 2.3%
Plutonium Jezebel (Center)	10/23/1973	4.071E+12 ± 3.5%	4.074E+12 ± 2.4%
Big-10 (Center)	7/9/1974	1.028E+12 ± 3.5%	1.036E+12 ± 2.4%

Current calculated cross section ratios for key iridium, plutonium and uranium isotopes are presented in Table 5-2 for experiments performed in the center of the critical assembly. Results from the traverse experiments of the oralloy core Flattop assembly are given in Table 5-3. A graphical representation of the span of the measured data is provided in Figure 5-1 indicating the Jezebel critical assembly with a plutonium core as having the hardest neutron fluence.

Table 5-2 Current calculated cross section ratios for center located experiments.

	Date of Irradiation	$\frac{N_{193m}}{N_{192}}$	$\frac{\sigma^{238_U}_{(n,f)}}{\sigma^{235_U}_{(n,f)}}$	$\frac{\sigma^{239_{Pu}}_{(n,f)}}{\sigma^{235_U}_{(n,f)}}$
Plutonium Core Flattop (Center)	8/10/1967	-	-	1.401 ± 3.5%
Oralloy Core Flattop (Center)	4/29/1968	-	-	1.378 ± 3.5%
Oralloy Core Flattop (Center)	4/7/1969	1.247 ± 1.6%	-	-
Plutonium Core Flattop (Center)	8/5/1970	1.597 ± 1.6%	-	-
Plutonium Jezebel (Center)	10/23/1973	2.220 ± 1.6%	0.211 ± 3.5%	-
Big-10 (Center)	1/27/1976	0.301 ± 1.6%	-	-

Table 5-3 Current calculated cross section ratios for the Flattop critical assembly traverse experiment performed on 8/18/1970 with an oralloy core.

Distance from Center [cm]	$\frac{N_{193m}}{N_{192}}$	$\frac{\sigma^{238_U}_{(n,f)}}{\sigma^{235_U}_{(n,f)}}$
0.875	1.342 ± 1.6%	0.151 ± 3.6%
1.11	1.313 ± 1.6%	0.148 ± 3.6%
3.54	1.213 ± 1.6%	0.145 ± 3.6%
5.05	1.038 ± 1.6%	0.132 ± 3.6%
5.72	0.897 ± 1.6%	0.114 ± 3.6%
8.2	0.397 ± 1.6%	0.058 ± 3.6%
10.82	0.259 ± 1.6%	0.036 ± 3.6%
14.63	0.176 ± 1.6%	0.022 ± 3.6%

All data reported are determined using modern K-factors from the appropriate time period, reassessed fission factors as conveyed in the previous section and reported mass spectrometry measurements. Uncertainties are propagated from counting and mass spectrometry errors and statistical errors from multiple measurements. Counting errors were not widely reported which required estimations. Iridium ratio uncertainties are largely dependent on the error assumed for the measured counts. A relative error was quoted for the measurement taken during the experiment performed in 4/7/1969. This is assumed for all iridium measurements since no other value was quoted. Mass spectrometry summaries reported uncertainties and these were propagated to the determination of the number of atoms in a sample. K-factor uncertainties are largely based on the statically determined error for the self-attenuated corrected ^{99}Mo K-factor for ^{235}U and quoted uncertainties for Q-values from the report by Selby et al [5]. Fission factor uncertainties are also determined in this manner and were determined to be a fraction of a percent. It is established the largest source of uncertainly is the K-factor.

Unfortunately iridium foils were not included in traverse of the Flattop assembly with an oralloy core experiment in 1971 that included both plutonium and uranium foils. A relationship between of the uranium and plutonium fission cross sections is desired. A function is developed relating the distance from center and the iridium ratio from data collected in 1970 from the traverse of the Flattop assembly with an oralloy core. It is determined that two fitting functions are necessary to describe the behavior. Historically the break between fitting functions is a distance of 8 cm. There is no compelling reason not to continue this reasoning. Figure 5-2 graphically presents the iridium spectral index as a function of distance from center from the oralloy core in the Flattop assembly. Using the fitting function the spectral index was calculated at the distance of the plutonium foils and the results are provided in Table 5-4.

Table 5-4 Current calculated cross section ratio for ^{239}Pu to ^{235}U for the Flattop critical assembly traverse experiment performed on 4/19/1971 with an oralloy core. Distance is from center. The iridium spectral index is calculated using fitting functions from the 1970 Flattop critical assembly experiment with an oralloy core.

Distance from Center [cm]			
^{239}Pu Foils	**^{235}U Foils**	$\frac{\sigma^{239_{Pu}}_{(n,f)}}{\sigma^{235_{U}}_{(n,f)}}$	$\frac{N_{193m}}{N_{192}}$
0.60	0.80	1.341 ± 3.5%	1.311 ± 2%
4.80	4.90	1.412 ± 3.5%	1.056 ± 2%
1.2	1.0	1.385 ± 3.5%	1.333 ± 2%
4.1	3.9	1.358 ± 3.5%	1.155 ± 2%
5.1	5.0	1.321 ± 3.5%	1.009 ± 2%
8.3	8.1	1.248 ± 3.5%	0.389 ± 2%
11.2	11.0	1.232 ± 3.5%	0.246 ± 2%
15.5	15.3	0.043 ± 3.5%	0.168 ± 2%

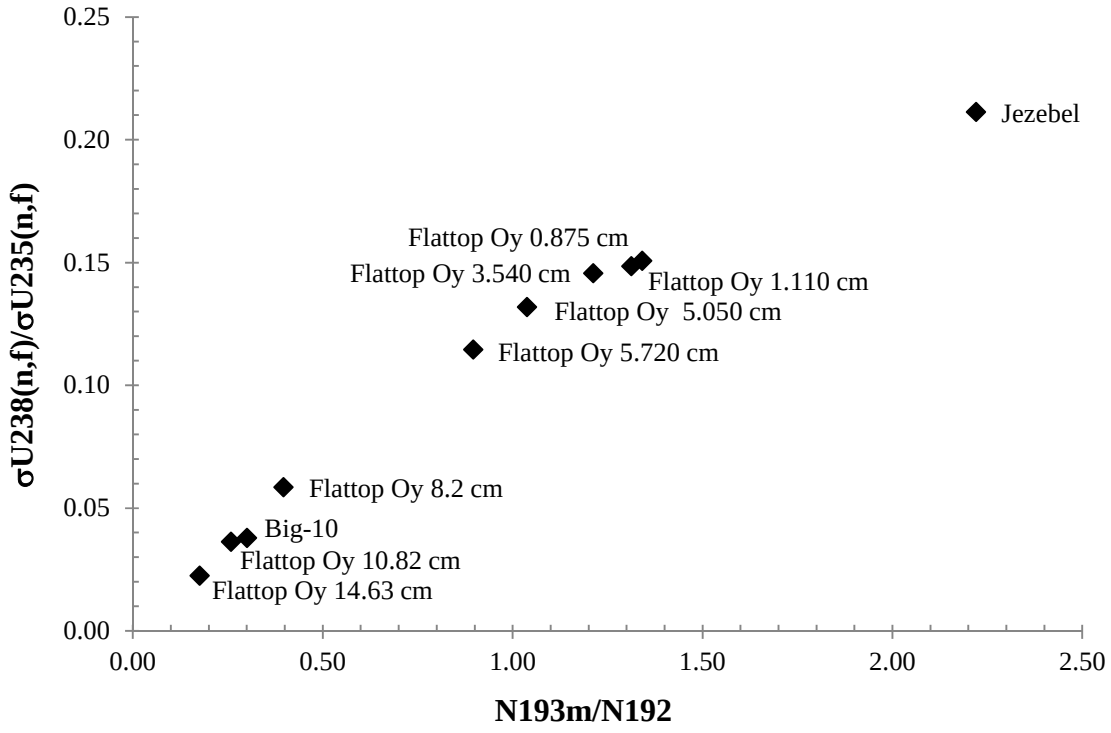

Figure 5-1 Re-evaluated uranium fission ratios and iridium spectral index for Pajarito critical assembly experiments performed during the late 1960's and early 1970's.

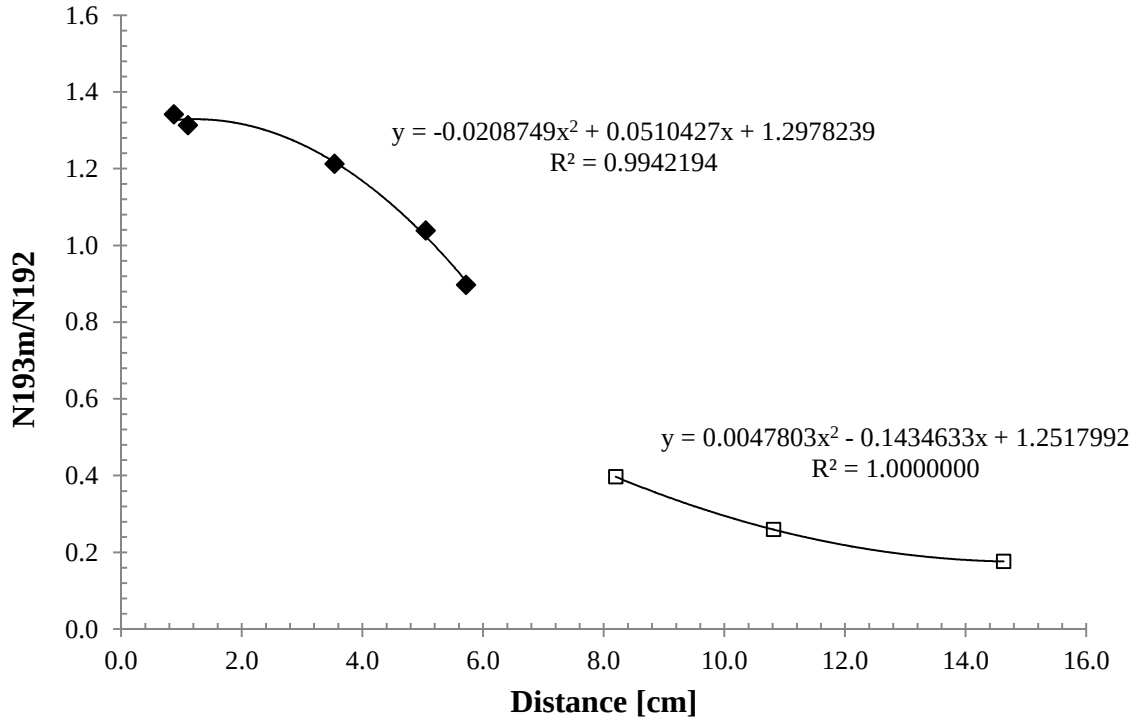

Figure 5-2 Iridium spectral index as a function of distance from center in the Flattop critical assembly with an oralloy core is plotted. The fitting function for distances greater than and less than 8 cm is provided. Data was collected from the 1970 experiment.

— 6 — Computation of Fission Spectrum Cross Sections from ENDF Libraries

In order to fully understand the behavior of neutron reaction cross sections across the fission energy spectrum it is necessary to compare observed data to published cross section data accepted by the nuclear data community. ENDF (Evaluated Nuclear Data File) is such a resource and has been extensively contributed to by LANL scientists. The most recent version is ENDF/B-VII.1 released in 2011 [7]. This database contains a combination of experimentally measured data and predictions from nuclear model calculations. The current cross section library utilized in IPC was first complied in 1992 using ENDF/B-VI data. Since that time a few revisions have been made but a full end-to-end evaluation using the ENDF/B-VII.1 data suite has not been executed. The following discussion is an overview of the process followed in 1992 of combining ENDF/B-VI data and critical assembly measurements to create a cross section library for IPC. This process is followed with the ENDF/B-VII.1 dataset for key isotopes required to form the basis of the IPC cross section library. Comparisons between the two datasets will be discussed. The intent is to discern if ENDF/B-VII.1 data and recent critical assembly measurements warrant updates to the IPC cross section library.

ENDF provides continuous cross section data across a full energy range. It is computationally challenging to perform calculations using the fully detailed ENDF data. Continuous energy Monte Carlo codes like MCNP are used for such applications. For the simple fluence based rate equations of IPC, difficulty is reduced by splitting the energy continuum into energy bins or groups. It is further simplified by evaluating neutron reactions in the fission and fast spectrum separately from reactions at lower energies.

The LANL 30-group structure was employed in the 1992 evaluation. This is still a well-used grouping for fusion problems as it covers the full energy range. A great deal of research and work has been accomplished in investigating varying number of groups within various codes and applications. Given that IPC solves the integral problem across the full energy spectrum it is felt the LANL 30-group structure is appropriate. Increasing the number of groups can mask errors in an assumed flux profile, but in return may result in the magnification of other uncertainties. The breakdown of the LANL 30-group structure is given in Table 6-1.

Cross sections are averaged across each energy bin. In order to calculate the average knowledge of the flux profile is required. An approximation of the shape of the flux profile is determined. A weight function is applied to account for the changes in the shape between groups within the fission energy spectrum. For uranium isotopes a weighting function based on the Big-10 critical assembly was applied. The weighting function for plutonium isotopes was based on the Flattop critical assembly with a plutonium core. R.E. MacFarlane of T-division at LANL was tasked with developed the weighting function for the 1992 evaluation. Recent work by A.C. Kahler of T-division generated the LANL 30-group structure for uranium, plutonium and iridium isotopes using ENDF/B-VII.1 libraries. Flux profiles from the Flattop, Big-10, Jezebel and Godiva critical assemblies applied are from Monte Carlo evaluations. There is no significant difference in results between critical assembly flux profiles as shown for ^{235}U in Figure 6-1. The same is true for plutonium and iridium isotopes and is presented in Appendix A: ENDF Data. However since the data is available, the collapse of the ENDF/B-VII.1 cross sections is performed with the appropriate critical assembly flux profile and NJOY weighting function.

ENDF libraries report data encoded in a computer readable format, so a nuclear data processing code is used to convert the data into a more usable format. NJOY [8], developed at LANL, is utilized for this purpose. NJOY runs were completed for the suite of uranium, plutonium and iridium isotopes using the appropriate weighting functions. Neutron reaction data selected to be processed by NJOY for uranium and plutonium are (n,γ), (n,f), (n,2n) and (n,3n). Reactions for iridium are (n,γ) and (n,n').

A FORTRAN code was developed during the 1992 evaluation to manipulate NJOY outputs into a form that could be used to compare to the experimental data. That code was rewritten using Python for this evaluation. The first step was to generate data files containing ENDF averaged

cross sections for each isotope and neutron reaction for each of the LANL 30-group energy bins. For plutonium, the isotopes of interest are ^{236}Pu to ^{244}Pu. Uranium isotopes of interest are ^{232}U to ^{240}U. Average cross sections for each of the 30 energy bins are plotted for ^{239}Pu and ^{235}U neutron reactions in Figure 6-2 and Figure 6-3 for both ENDF/B-VI and ENDF/B-VII.1. Iridium cross sections are plotted in Figure 6-4 and Figure 6-5.

Table 6-1 LANL 30-Group Structure

Group	Energy Bin [eV]		
1	1.390E-04	-	1.520E-01
2	1.520E-01	-	4.140E-01
3	4.140E-01	-	1.130E+00
4	1.130E+00	-	3.060E+00
5	3.060E+00	-	8.320E+00
6	8.320E+00	-	2.260E+01
7	2.260E+01	-	6.140E+01
8	6.140E+01	-	1.670E+02
9	1.670E+02	-	4.540E+02
10	4.540E+02	-	1.235E+03
11	1.235E+03	-	3.350E+03
12	3.350E+03	-	9.120E+03
13	9.120E+03	-	2.480E+04
14	2.480E+04	-	6.760E+04
15	6.760E+04	-	1.840E+05
16	1.840E+05	-	3.030E+05
17	3.030E+05	-	5.000E+05
18	5.000E+05	-	8.230E+05
19	8.230E+05	-	1.353E+06
20	1.353E+06	-	1.738E+06
21	1.738E+06	-	2.232E+06
22	2.232E+06	-	2.865E+06
23	2.865E+06	-	3.680E+06
24	3.680E+06	-	6.070E+06
25	6.070E+06	-	7.790E+06
26	7.790E+06	-	1.000E+07
27	1.000E+07	-	1.200E+07
28	1.200E+07	-	1.350E+07
29	1.350E+07	-	1.500E+07
30	1.500E+07	-	1.700E+07

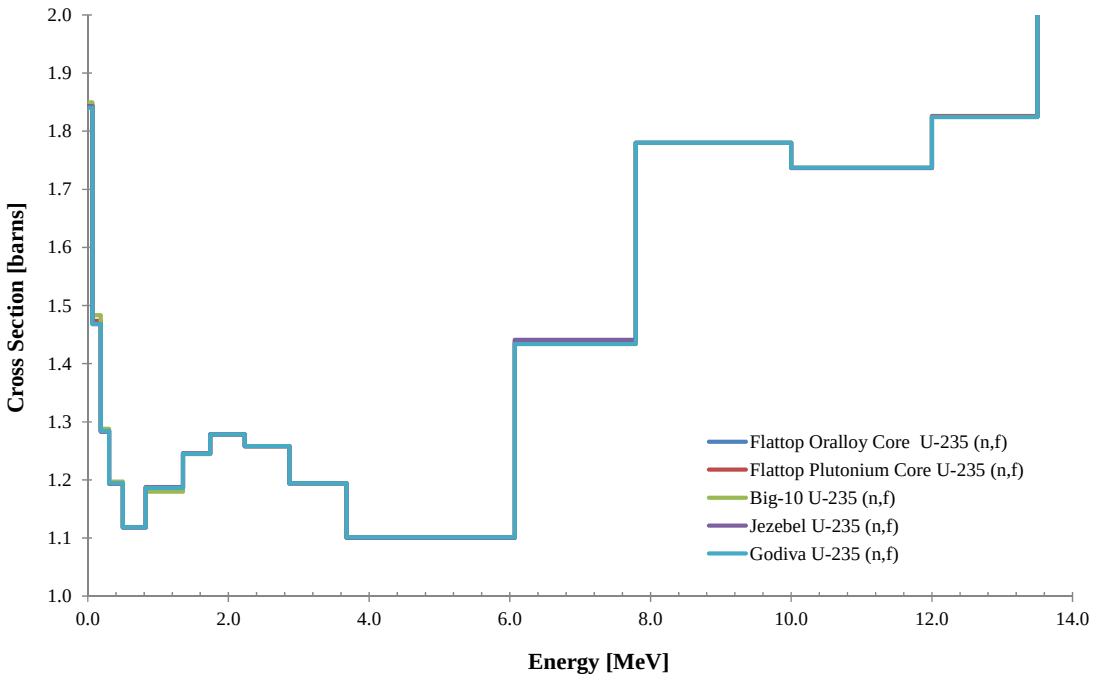

Figure 6-1 Comparison of the LANL 30-group structure for the isotope ^{235}U fission cross section between critical assembly flux profiles is shown.

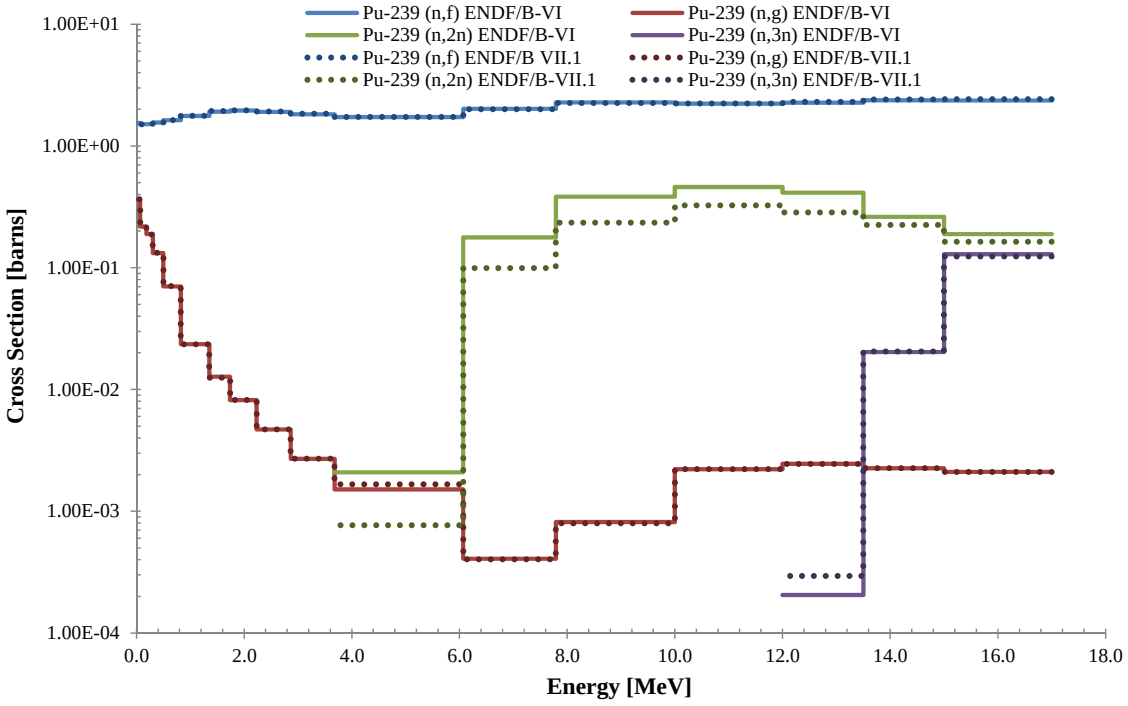

Figure 6-2 Average cross section of ^{239}Pu neutron reactions across the LANL 30-group structure with a weighting function from the plutonium core Flattop critical assembly applied for ENDF/B-VI and ENDF/B-VII.1 data.

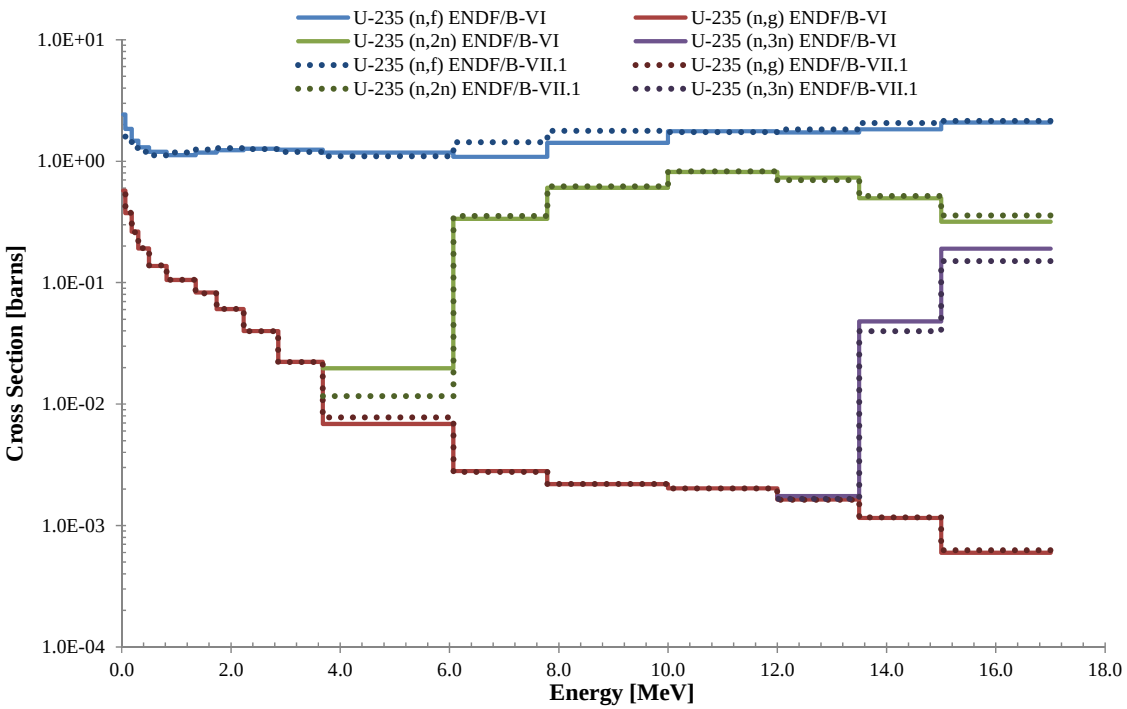

Figure 6-3 Average cross sections for ^{235}U neutron reactions across the LANL 30-group structure with a weighting function from the Big-10 critical assembly applied for ENDF/B-VI and ENDF/B-VII.1 data.

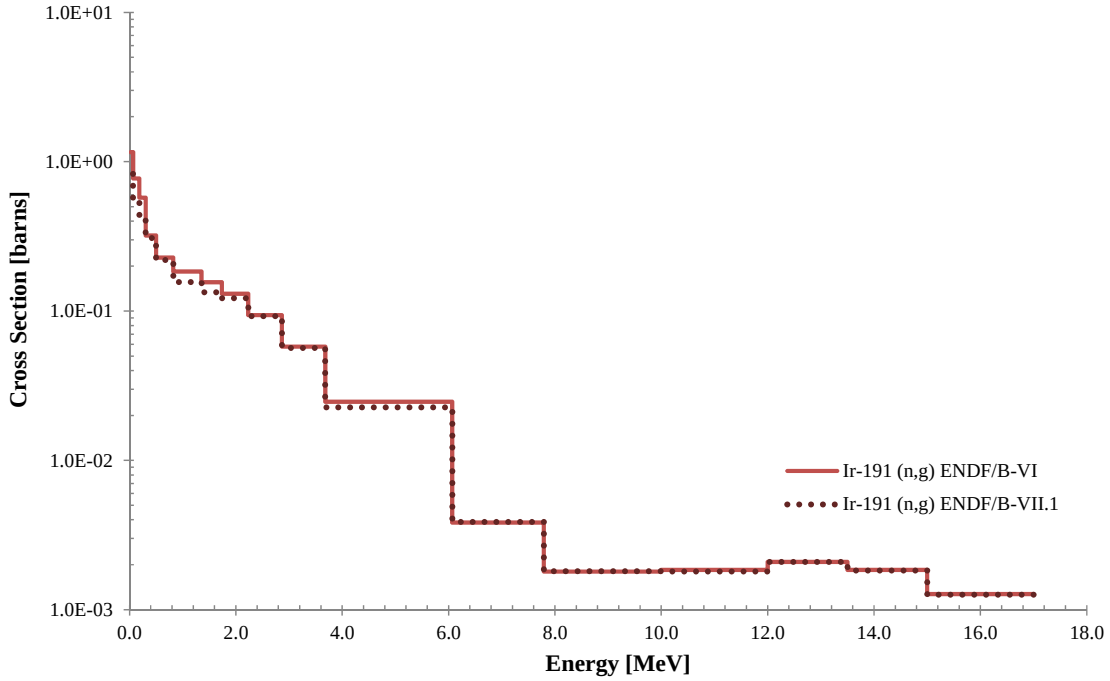

Figure 6-4 Average cross sections for ^{191}Ir neutron capture reactions across the LANL 30-group structure with a weighting function for the oralloy core Flattop critical assembly applied for ENDF/B-VI and ENDF/B-VII.1 data.

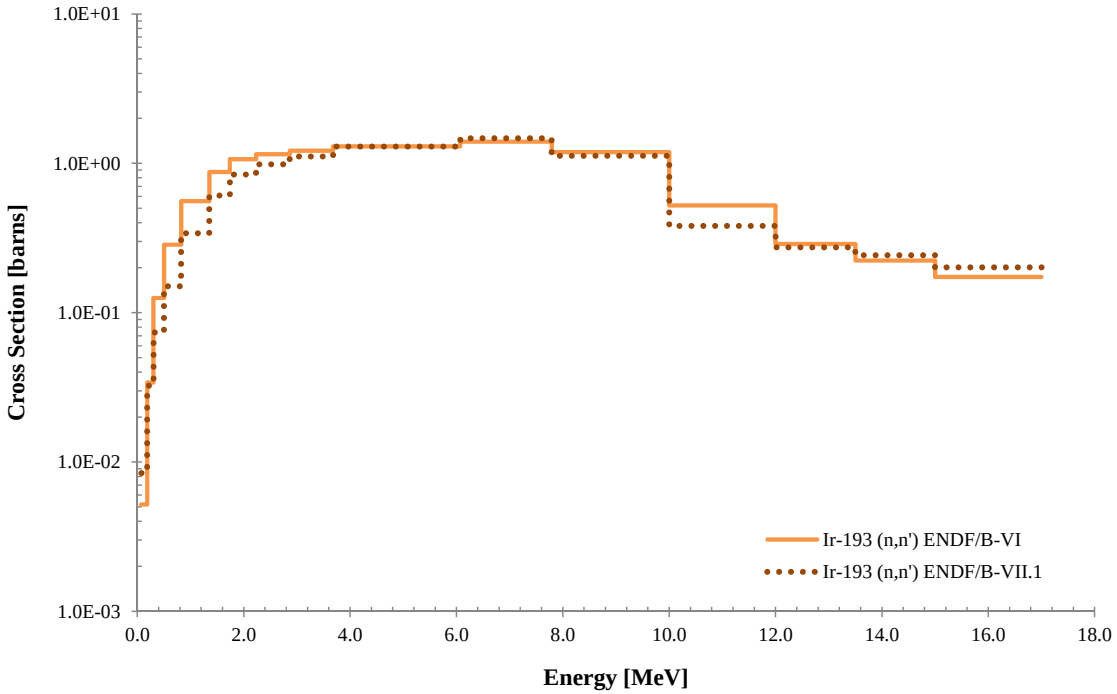

Figure 6-5 Average cross sections for ^{193}Ir inelastic neutron scattering capture reactions across the LANL 30-group structure with a weighting function for the oralloy core Flattop critical assembly applied for ENDF/B-VI and ENDF/B-VII.1 data.

6.1 Cross Section Collapse

Using the LANL 30-group cross section data, a collapse is performed to determine the average cross section at locations in the critical assemblies that measurements had been taken. Flux profiles for the Flattop, Jezebel, Godiva, Big-10 generated by T-division for the 1992 evaluation are plotted in Figure 6-6, Figure 6-7 and Figure 6-8. A virgin profile, a bare fully enriched uranium or plutonium core, in addition is utilized to provide a data point for hard spectrum and is shown in Figure 6-9. These historical flux profiles are applied for the current work.

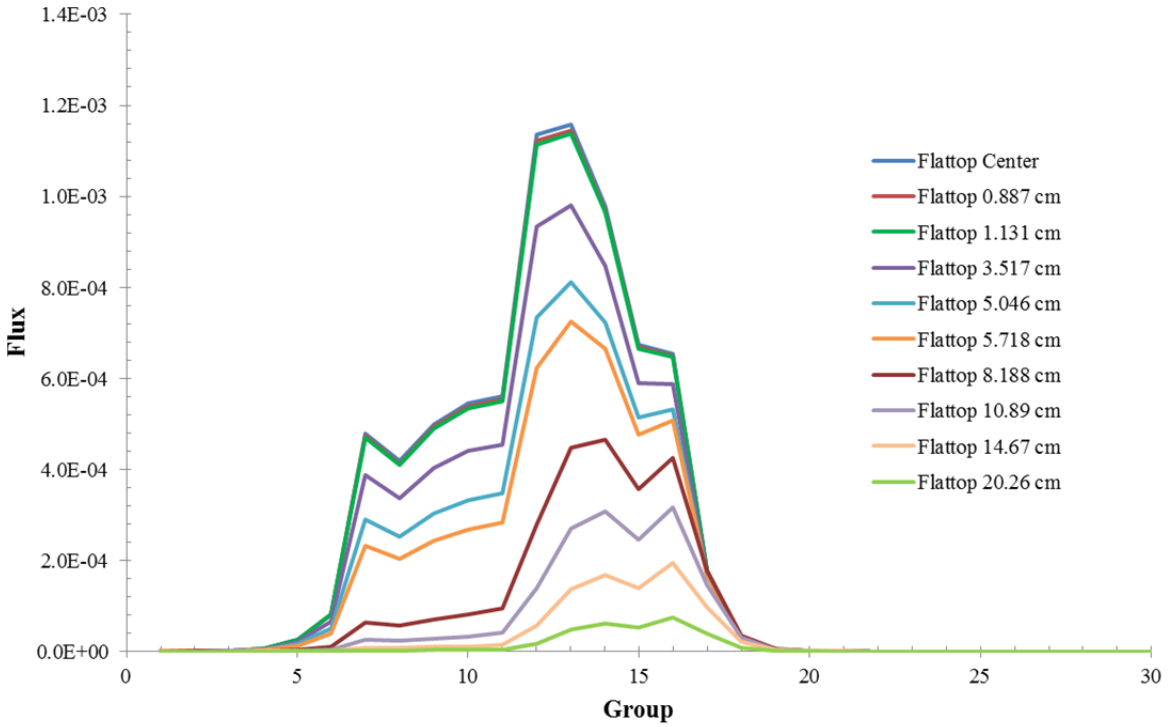

Figure 6-6 Oralloy Flattop flux profiles from varying distances from center are plotted.

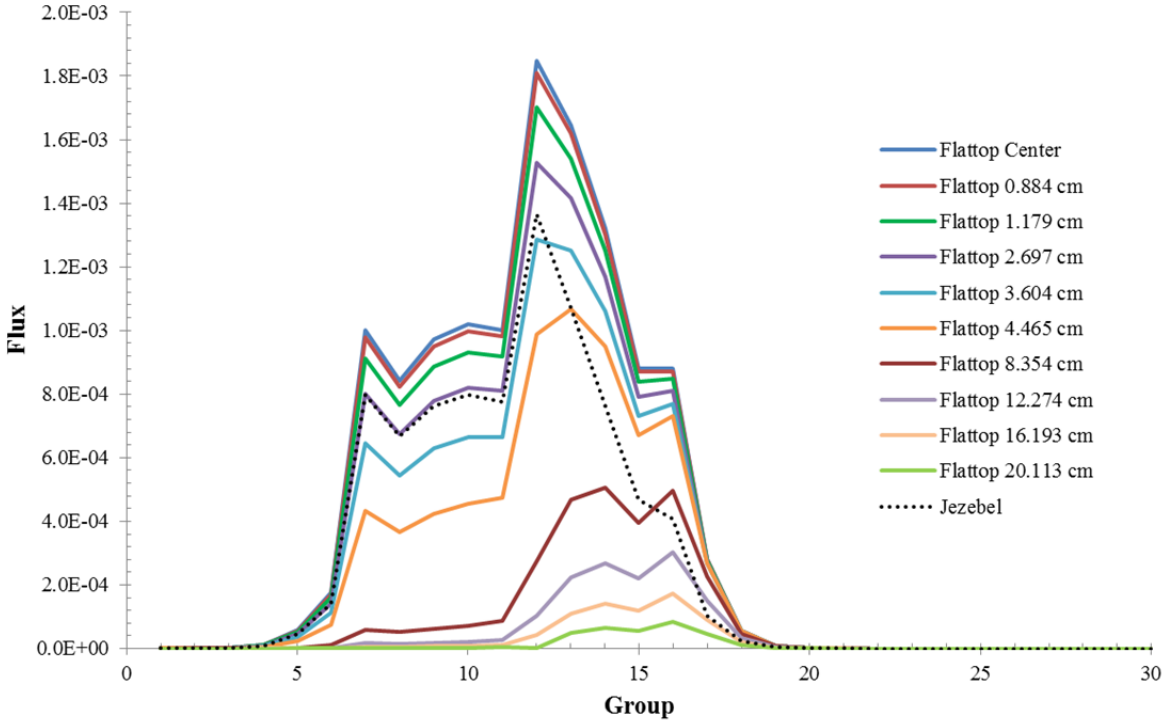

Figure 6-7 Plutonium Flattop flux profile from varying distances from center is plotted. Flux profile for a center location in the Jezebel assembly with a plutonium core is included.

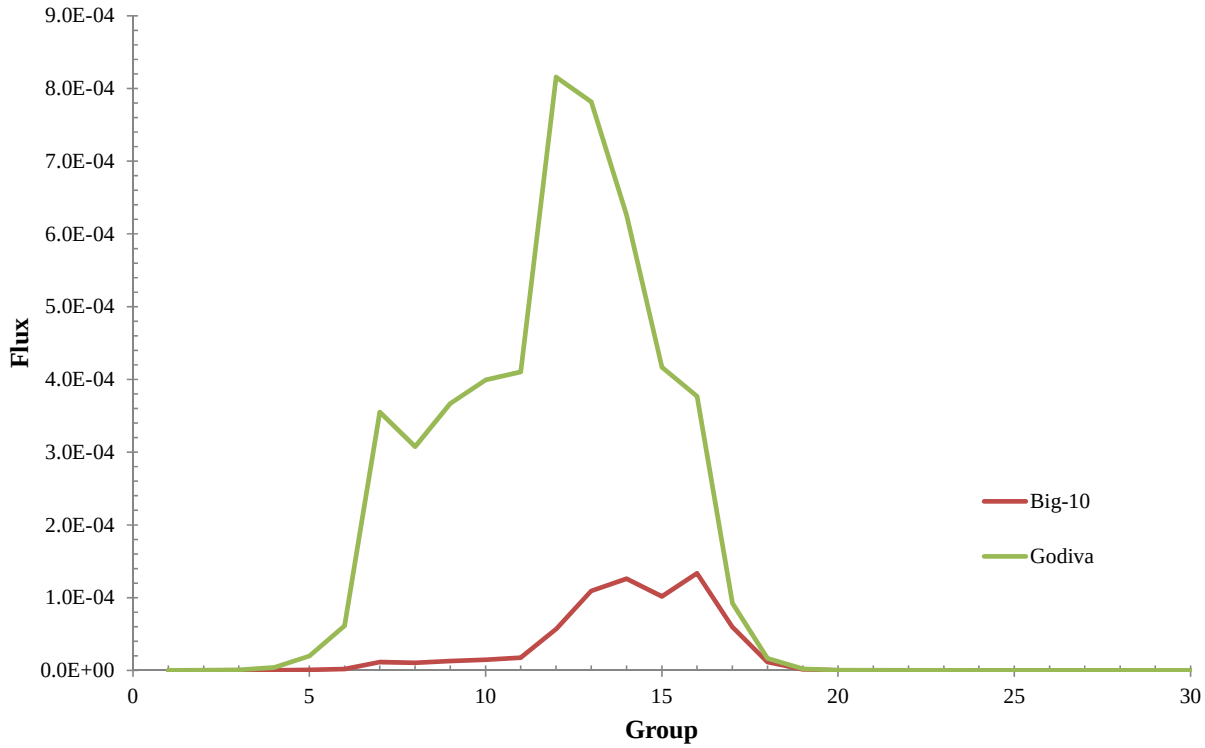

Figure 6-8 Center location flux profile for the Big-10 and Godiva assemblies with an oralloy core are plotted.

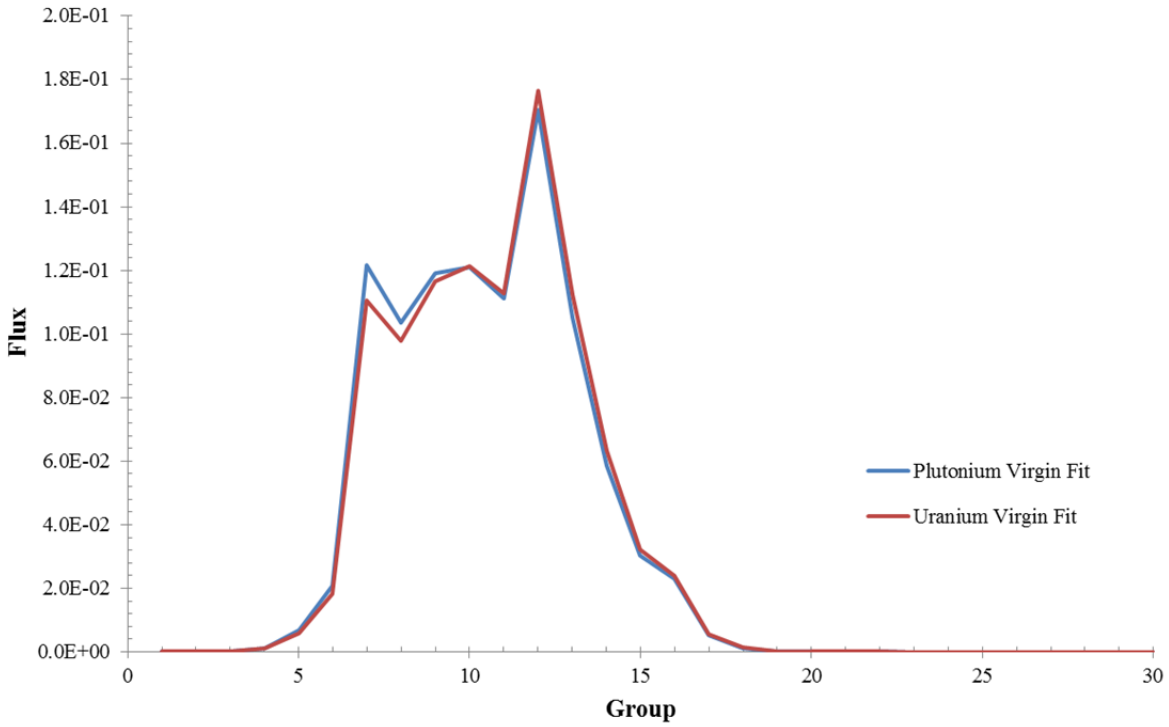

Figure 6-9 Virgin flux profiles for a uranium and plutonium core are plotted.

6.1.1 Summary of Cross Collapse

Collapsed average cross sections are determined by approximating Equation (6) by

$$\langle \sigma_{rxn}^{x} \rangle = \frac{\sum_{E}^{30} \phi(E)\sigma(E)}{\sum_{E}^{30} \phi(E)}. \tag{35}$$

Results based on ENDF/B-VI and ENDF/B-VII.1 data for key isotopes are given in Table 6-2 and Table 6-7. The percent difference is provided. It is evident that the iridium data between the two ENDF libraries is significant. During the 1992 evaluation it became apparent that the observed data and the predicated data from ENDF were not matching up. As result a modified data set for ^{191}Ir and ^{193}Ir was developed and used. This data is given in Table 6-8 and Table 6-9 which shows an improvement in the comparison to the ENDF/B-VII data. This data is plotted in Figure 6-10 and Figure 6-11.

Table 6-2 Cross section collapse for the ^{235}U neutron fission reaction at specific critical assembly locations based on ENDF/B-VI and ENDF/B-VII.1 data is given. Percent difference between the two data libraries is provided. Applied flux profile is based on the Big-10 critical assembly for ENDF/B-VI results. ENDF/B-VII.1 results applied the appropriate critical assembly flux profile and NJOY weighting function.

	ENDF/B-VI	**ENDF/B-VII.1**	
Critical Assembly	**σU-235(n,f)**	**σU-235(n,f)**	**% Diff**
Virgin Fits Uranium	1.2130	1.2211	0.67%
Jezebel Plutonium Core	1.2264	1.2332	0.55%
Godiva	1.2365	1.2409	0.36%
Flattop Oralloy Center	1.2453	1.2493	0.33%
Flattop Oralloy 0.887 cm	1.2455	1.2496	0.32%
Flattop Oralloy 1.131 cm	1.2457	1.2497	0.32%
Flattop Oralloy 3.517 cm	1.2498	1.2535	0.30%
Flattop Oralloy 5.046 cm	1.2578	1.2609	0.25%
Flattop Oralloy 5.718 cm	1.2652	1.2677	0.20%
Flattop Oralloy 8.188 cm	1.3105	1.3098	0.06%
Flattop Oralloy 10.89 cm	1.3430	1.3408	0.17%
Flattop Oralloy 14.67 cm	1.3746	1.3711	0.25%
Flattop Oralloy 20.26 cm	1.3941	1.3900	0.30%
Big-10	1.3403	1.3417	0.11%

Table 6-3 Cross section collapse for the ^{238}U neutron fission reaction at specific critical assembly locations based on ENDF/B-VI and ENDF/B-VII.1 data is given. Percent difference between the two data libraries is provided. Applied flux profile is based on the Big-10 critical assembly for ENDF/B-VI results. ENDF/B-VII.1 results applied the appropriate critical assembly flux profile and NJOY weighting function.

	ENDF/B-VI	ENDF/B-VII.1	
Critical Assembly	**σU-238(n,f)**	**σU-238(n,f)**	**% Diff**
Virgin Fits Uranium	0.3014	0.3069	1.81%
Jezebel Plutonium Core	0.2536	0.2598	2.43%
Godiva	0.1965	0.2013	2.38%
Flattop Oralloy Center	0.1817	0.1861	2.38%
Flattop Oralloy 0.887 cm	0.1813	0.1857	2.38%
Flattop Oralloy 1.131 cm	0.1811	0.1854	2.38%
Flattop Oralloy 3.517 cm	0.1745	0.1787	2.38%
Flattop Oralloy 5.046 cm	0.1610	0.1649	2.40%
Flattop Oralloy 5.718 cm	0.1476	0.1513	2.42%
Flattop Oralloy 8.188 cm	0.0760	0.0780	2.61%
Flattop Oralloy 10.89 cm	0.0490	0.0504	2.69%
Flattop Oralloy 14.67 cm	0.0316	0.0325	2.75%
Flattop Oralloy 20.26 cm	0.0223	0.0229	2.77%
Big-10	0.0537	0.0546	1.69%

Table 6-4 Cross section collapse for the ^{239}Pu neutron fission reaction at specific critical assembly locations based on ENDF/B-VI and ENDF/B-VII.1 data is given. Percent difference between the two data libraries is provided. Applied flux profile is based on the Big-10 critical assembly for ENDF/B-VI results. ENDF/B-VII.1 results applied the appropriate critical assembly flux profile and NJOY weighting function.

	ENDF/B-VI	ENDF/B-VII.1	
Critical Assembly	**σPu-239(n,f)**	**σPu-239(n,f)**	**% Diff**
Virgin Fits Uranium	1.7861	1.7907	0.26%
Godiva	1.7169	1.7233	0.37%
Flattop Oralloy Center	1.7050	1.7109	0.35%
Flattop Oralloy 0.887 cm	1.7047	1.7106	0.35%
Flattop Oralloy 1.131 cm	1.7045	1.7104	0.35%
Flattop Oralloy 3.517 cm	1.6995	1.7053	0.34%
Flattop Oralloy 5.046 cm	1.6894	1.6950	0.33%
Flattop Oralloy 5.718 cm	1.6798	1.6852	0.32%
Flattop Oralloy 8.188 cm	1.6272	1.6314	0.26%
Flattop Oralloy 10.89 cm	1.6038	1.6078	0.25%
Flattop Oralloy 14.67 cm	1.5872	1.5910	0.24%
Flattop Oralloy 20.26 cm	1.5777	1.5815	0.24%
Big-10	1.6053	1.6070	0.11%

Table 6-5 Cross section collapse for the ^{239}Pu neutron fission reaction at specific critical assembly locations based on ENDF/B-VI and ENDF/B-VII.1 data is given. Percent difference between the two data libraries is provided. Applied flux profile is based on the Flattop critical assembly with a plutonium core for ENDF/B-VI results. ENDF/B-VII.1 results applied the appropriate critical assembly flux profile and NJOY weighting function.

	ENDF/B-VI	**ENDF/B-VII.1**	
Critical Assembly	**σPu-239(n,f)**	**σPu-239(n,f)**	**% Diff**
Virgin Fits Plutonium	1.7900	1.7989	0.50%
Jezebel Plutonium Core	1.7517	1.7601	0.48%
Flattop Plutonium Center	1.7275	1.7349	0.42%
Flattop Plutonium 0.884 cm	1.7269	1.7342	0.42%
Flattop Plutonium 1.790 cm	1.7246	1.7319	0.42%
Flattop Plutonium 2.697 cm	1.7201	1.7272	0.41%
Flattop Plutonium 3.604 cm	1.7113	1.7183	0.40%
Flattop Plutonium 4.465 cm	1.6920	1.6985	0.38%
Flattop Plutonium 8.354 cm	1.6177	1.6226	0.30%
Flattop Plutonium 12.274 cm	1.5933	1.5979	0.29%
Flattop Plutonium 16.193 cm	1.5817	1.5861	0.28%
Flattop Plutonium 20.113	1.5673	1.5720	0.30%

Table 6-6 Cross section collapse for the ^{191}Ir neutron capture reaction at specific critical assembly locations based on ENDF/B-VI and ENDF/B-VII.1 data is given. Percent difference between the two data libraries is provided. Applied flux profile is based on the Big-10 critical assembly for ENDF/B-VI results. ENDF/B-VII.1 results applied the appropriate critical assembly flux profile and NJOY weighting function.

	ENDF/B-VI	**ENDF/B-VII.1**	
Critical Assembly	**σIr-191(n,γ)**	**σIr-191(n,γ)**	**% Diff**
Virgin Fits Uranium	0.1797	0.1583	12.6%
Godiva	0.2758	0.2308	16.5%
Flattop Oralloy Center	0.2981	0.2480	17.7%
Flattop Oralloy 0.887 cm	0.2987	0.2485	18.3%
Flattop Oralloy 1.131 cm	0.2990	0.2487	18.4%
Flattop Oralloy 3.517 cm	0.3090	0.2563	18.4%
Flattop Oralloy 5.046 cm	0.3289	0.2715	18.6%
Flattop Oralloy 5.718 cm	0.3477	0.2858	19.1%
Flattop Oralloy 8.188 cm	0.4572	0.3693	19.5%
Flattop Oralloy 10.89 cm	0.5219	0.4180	21.3%
Flattop Oralloy 14.67 cm	0.5791	0.4609	22.1%
Flattop Oralloy 20.26 cm	0.6138	0.4869	22.7%
Big-10	0.5152	0.4169	23.1%

Table 6-7 Cross section collapse for the ^{193}Ir inelastic neutron scatter reaction at specific critical assembly locations based on ENDF/B-VI and ENDF/B-VII.1 data is given. Percent difference between the two data libraries is provided. Applied flux profile is based on the Big-10 critical assembly for ENDF/B-VI results. ENDF/B-VII.1 results applied the appropriate critical assembly flux profile and NJOY weighting function.

	ENDF/B-VI	**ENDF/B-VII.1**	
Critical Assembly	**σIr-193(n,n')**	**σIr-193(n,n')**	**% Diff**
Virgin Fits Uranium	0.7966	0.6498	20.3%
Godiva	0.5785	0.4595	22.9%
Flattop Oralloy Center	0.5431	0.4293	23.4%
Flattop Oralloy 0.887 cm	0.5422	0.4285	23.4%
Flattop Oralloy 1.131 cm	0.5417	0.4280	23.4%
Flattop Oralloy 3.517 cm	0.5264	0.4150	23.7%
Flattop Oralloy 5.046 cm	0.4954	0.3885	24.2%
Flattop Oralloy 5.718 cm	0.4653	0.3624	24.9%
Flattop Oralloy 8.188 cm	0.3010	0.2215	30.5%
Flattop Oralloy 10.89 cm	0.2298	0.1636	33.6%
Flattop Oralloy 14.67 cm	0.1786	0.1237	36.3%
Flattop Oralloy 20.26 cm	0.1495	0.1014	38.4%
Big-10	0.2377	0.1684	34.1%

Table 6-8 Cross section collapse for the ^{191}Ir neutron capture reaction at specific critical assembly locations based on Drake modified ENDF/B-VI and ENDF/B-VII.1 data is given. Percent difference between the two data libraries is provided. Applied flux profile is based on the Big-10 critical assembly for ENDF/B-VI results. ENDF/B-VII.1 results applied the appropriate critical assembly flux profile and NJOY weighting function.

	Drake Modified ENDF/B-VI	**ENDF/B-VII.1**	
Critical Assembly	**σIr-191(n,γ)**	**σIr-191(n,γ)**	**% Diff**
Virgin Fits Uranium	0.1621	0.1583	2.34%
Godiva	0.2437	0.2308	5.41%
Flattop Oralloy Center	0.2624	0.2480	5.63%
Flattop Oralloy 0.887 cm	0.2629	0.2485	5.64%
Flattop Oralloy 1.131 cm	0.2632	0.2487	5.65%
Flattop Oralloy 3.517 cm	0.2717	0.2563	5.82%
Flattop Oralloy 5.046 cm	0.2886	0.2715	6.13%
Flattop Oralloy 5.718 cm	0.3047	0.2858	6.39%
Flattop Oralloy 8.188 cm	0.3983	0.3693	7.56%
Flattop Oralloy 10.89 cm	0.4535	0.4180	8.16%
Flattop Oralloy 14.67 cm	0.5025	0.4609	8.64%
Flattop Oralloy 20.26 cm	0.5322	0.4869	8.90%
Big-10	0.4471	0.4169	6.98%

Table 6-9 Cross section collapse for the ^{193}Ir inelastic neutron scattering reaction at specific critical assembly locations based on MacInnes modified ENDF/B-VI and ENDF/B-VII.1 data is given. Percent difference between the two data libraries is provided. Applied flux profile is based on the Big-10 critical assembly for ENDF/B-VI results. ENDF/B-VII.1 results applied the appropriate critical assembly flux profile and NJOY weighting function.

	MacInnes Modified ENDF/B-VI	**ENDF/B-VII.1**	
Critical Assembly	**σIr-193(n,n')**	**σIr-193(n,n')**	**% Diff**
Virgin Fits Uranium	0.7157	0.6498	9.65%
Godiva	0.5025	0.4595	8.95%
Flattop Oralloy Center	0.4699	0.4293	9.03%
Flattop Oralloy 0.887 cm	0.4691	0.4285	9.03%
Flattop Oralloy 1.131 cm	0.4685	0.4280	9.03%
Flattop Oralloy 3.517 cm	0.4543	0.4150	9.04%
Flattop Oralloy 5.046 cm	0.4253	0.3885	9.05%
Flattop Oralloy 5.718 cm	0.3968	0.3624	9.06%
Flattop Oralloy 8.188 cm	0.2430	0.2215	9.26%
Flattop Oralloy 10.89 cm	0.1796	0.1636	9.27%
Flattop Oralloy 14.67 cm	0.1355	0.1237	9.14%
Flattop Oralloy 20.26 cm	0.1109	0.1014	9.01%
Big-10	0.1879	0.1684	10.94%

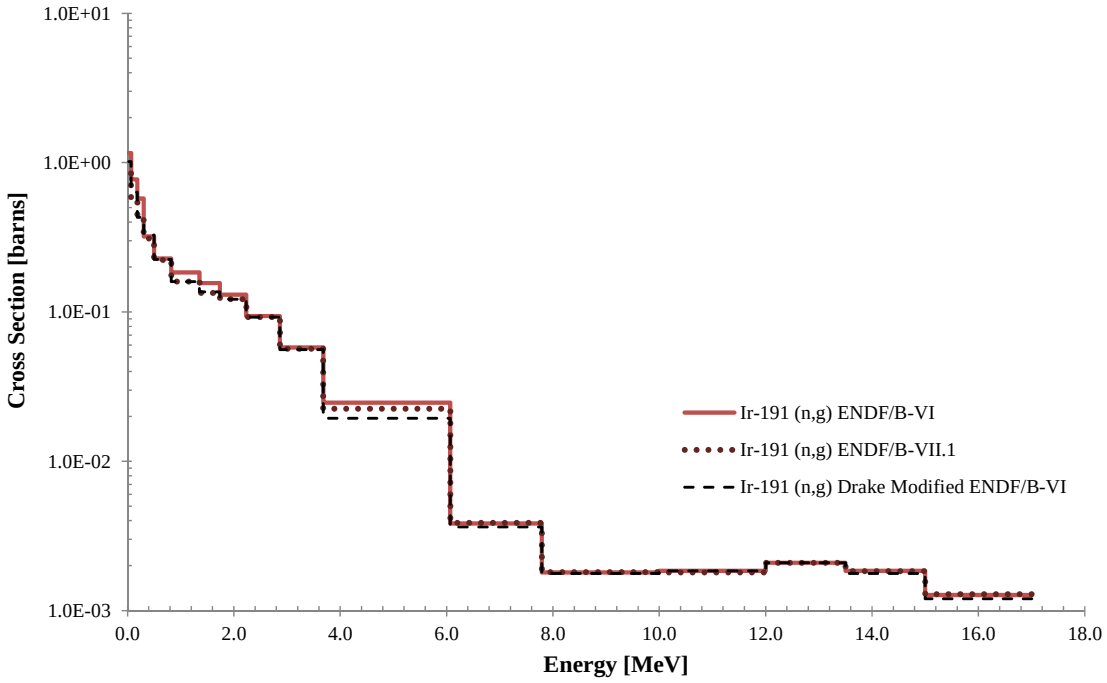

Figure 6-10 Average cross sections for ^{191}Ir neutron capture reactions across the LANL 30-group structure with a weighting function for the oralloy core Big-10 critical assembly applied for ENDF/B-VI, ENDF/B-VII.1 and Drake modified ENDF/B-VI data.

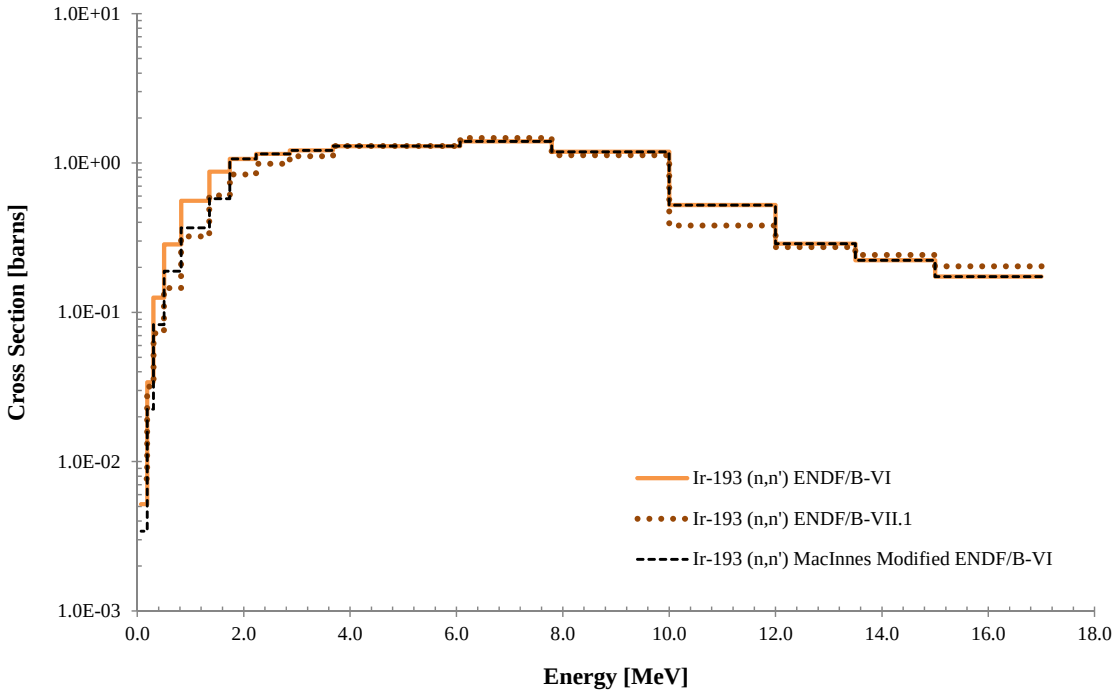

Figure 6-11 Average cross sections for ^{193}Ir inelastic neutron scattering capture reactions across the LANL 30-group structure with a weighting function for the oralloy core Big-10 critical assembly applied for ENDF/B-VI, ENDF/B-VII.1 and MacInnes modified data.

— 7 — Modification of ENDF Iridium Cross Sections

M.R MacInnes investigated the iridium production cross sections as part of the 1992 evaluation [9]. As with the actinide cross sections, average cross sections are calculated for each of the LANL 30-groups based on an assumed flux profile across the full energy spectrum. Data from ENDF/B-VI for the ^{191}Ir (n,γ)^{192}Ir reaction was compared to a dataset that was modified by Drake et al [9]. D.W. Barr communicated that this modification formulated by Drake and reported by R. Seamon [9] in a memo is an improvement over the ENDF/B-VI data. The behavior of the capture reaction of ^{191}Ir to the fission cross section of ^{235}U against the uranium fission ratio is shown in Figure 7-1. It is evident the modification done by Drake did move the calculated data closer to the measured values as did ENDF/B-VII.1 data. Historically a curve is fit to the ENDF data and the ^{191}Ir(n,γ)^{192}Ir cross section is raised to match the observed data points. This process is repeated for the ENDF/B-VII.1 data as shown in Figure 7-2. The modification factor used historically is 1.033 compared to 1.0737 determined for the ENDF/B-VII.1 dataset. A program, developed in Python for this work, is utilized to minimize chi-squared between the modified ENDF/B-VII.1 data and the observed data. As a result an improved method of determining the modification factor is acquired. Curve fitting is performed without the calculated virgin data points to ensure that the fit it not unnecessarily skewed since there are no measured data points in this region.

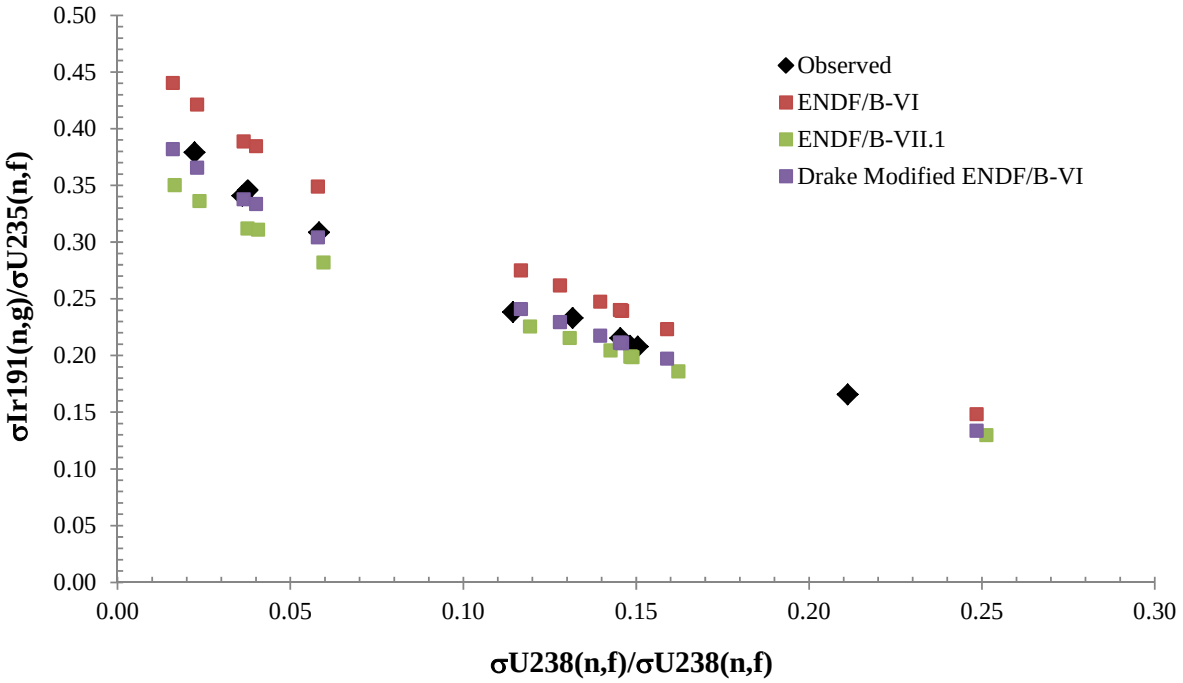

Figure 7-1 Behavior of the ^{191}Ir capture cross section to the uranium fission cross section ratio is plotted. Data for the Drake modification was taken from the MacInnes evaluation in 1992.

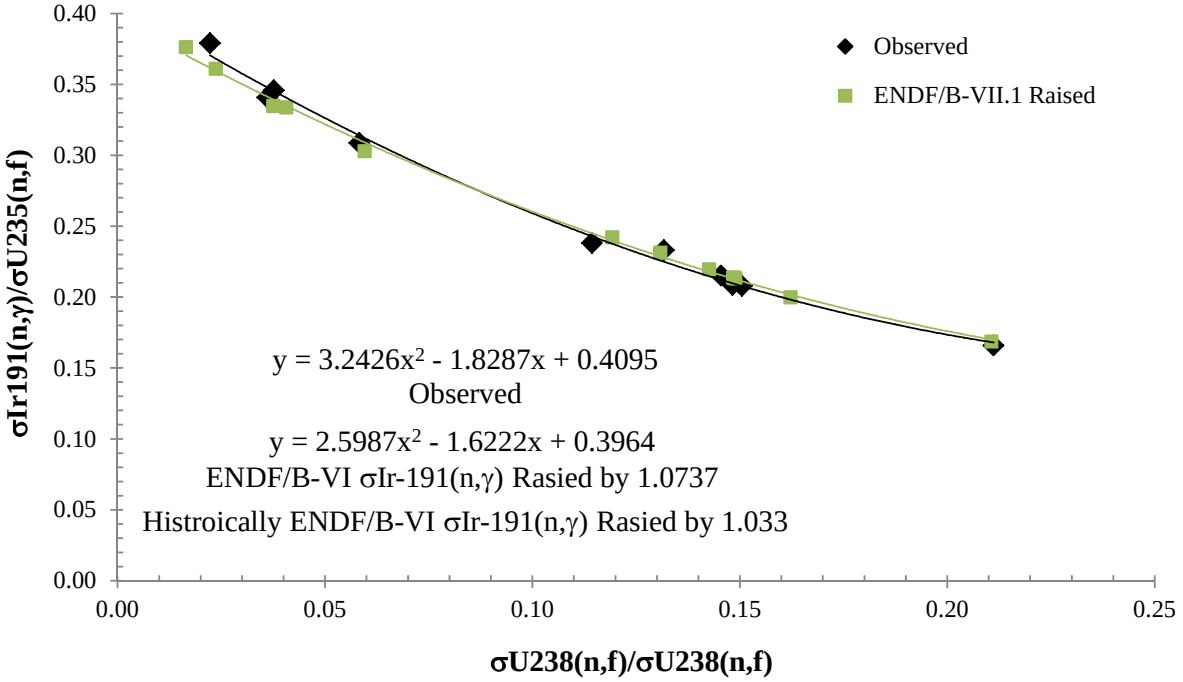

Figure 7-2 Curve fits of the observed data and ENDF/B-VII calculated data is plotted. ENDF/B-VII ^{191}Ir(n,g) data has been raised by 1.0737 to move the curve to fit to the observed data. Historically the Drake modified ENDF/B-VI data was raised by 1.033. Calculated virgin data points are not included.

Modifications to the $^{193}Ir(n,n')^{193m}Ir$ cross section data is required to match the observed data. MacInnes by trial and error determine a 1.514 reduction in the averaged cross section data for energy groups 11 to 16 was required [9]. This reduction is apparent in Figure 6-11. The ratio of the inelastic cross section for ^{193}Ir to the fission cross section of ^{235}U plotted against the uranium fission cross ratio is given in Figure 7-3. ENDF/B-VII.1 calculated data is an improvement over the previous calculated datasets as compared to the observed values. There still remains a significant discrepancy between the calculated and measured data points. A curve is fit to the calculated data and then the ^{193}Ir inelastic cross section is reduced to fit the observed data. This reduction is shown in Figure 7-4.

Comparison of the iridium spectral index, N193m/N192, to the uranium fission cross section ratio is given in Figure 7-4. As it is evident with the ^{193}Ir inelastic cross section there is a distinction between the ENDF data and the measured data. A bias of approximately a factor of two is known to exist due to the procedure followed to measure the counts from the iridium foils after irradiation in the critical assemblies. By reducing the calculated iridium spectral index a factor of 2.2682 for ENDF/B-VII data is determined. Historically this factor is 2.395. This factor is applied to the calculated iridium spectral index for both due to both an oralloy and plutonium core. Since there are an insufficient number of measurements conducted for assemblies with a plutonium core to perform a calculated to measured evaluation to determine an iridium reduction factor, the factor from the oralloy core based experiments is applied. Modified ENDF data is tabulated Table 7-1 and Table 7-2. The reduction factor determined using the ENDF/B-VII.1 dataset resulted in an improved fit to the measured data when compared to the ENDF/B-VI based fit. Figure 7-7 shows the fit to the modified ENDF/B-VI dataset.

Due to the known bias between the measured integral cross section from critical assembly experiments for iridium, a fit to the measured data is chosen for the IPC cross section library. The current fission cross section ratio of ^{238}U to ^{235}U as a function of the iridium spectral index is a polynomial fit to the measured data obtained from the critical assembly experiments. Historically a polynomial function is fit to the observed data on a log-log scale as shown in Figure 7-8. The variation in the historical fit and the current fit which uses the recent reevaluated data are due to discrepancies in assumed K-factors and different curve fitting programs. Excel and curve fitting routines from Python are used for the current work.

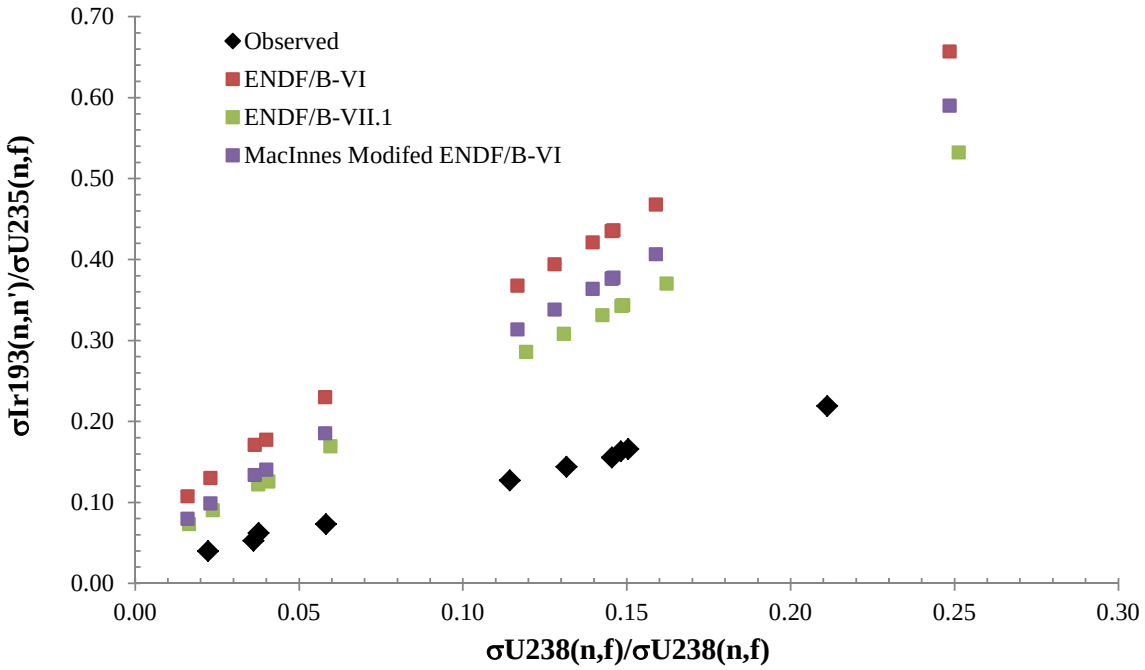

Figure 7-3 Behavior of the ^{193}Ir inelastic cross section to the uranium fission cross section ratio is plotted. Data for the modified ENDF/B-VI data is taken from the MacInnes evaluation in 1992.

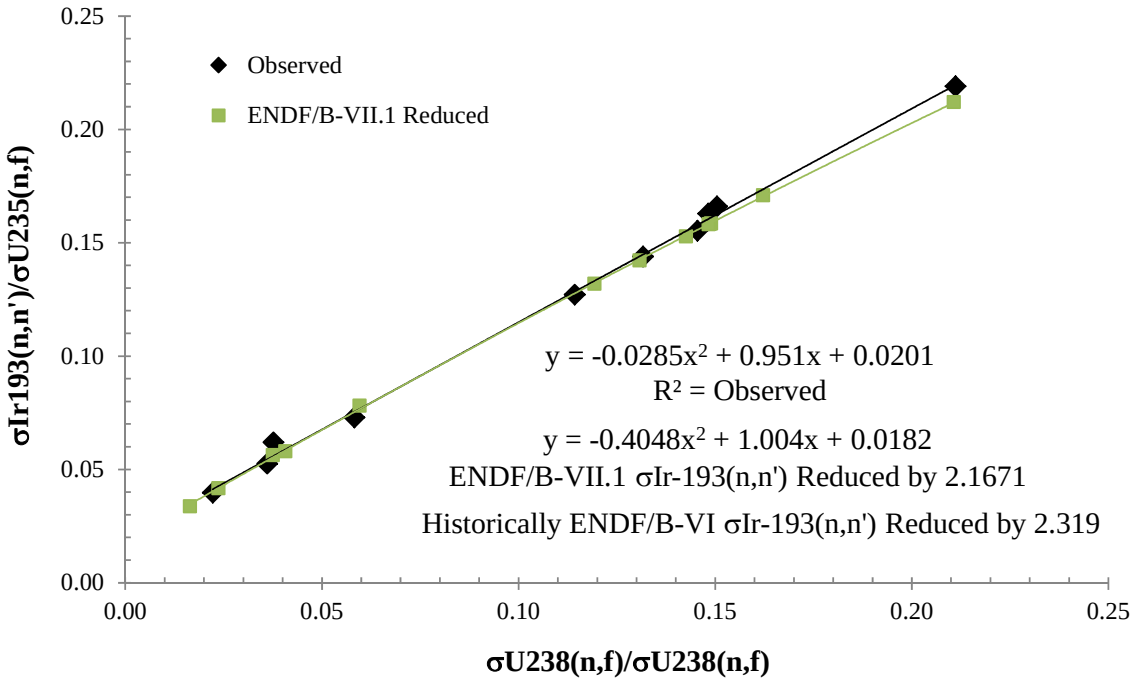

Figure 7-4 Curve fits of the observed data and ENDF/B-VII calculated data is plotted. ENDF/B-VII ^{193}Ir(n,n') data has been reduced by 2.1671 to move the curve to fit to the observed data. Historically the Drake modified ENDF/B-VI data was reduced by 2.319. Calculated virgin data points are not included.

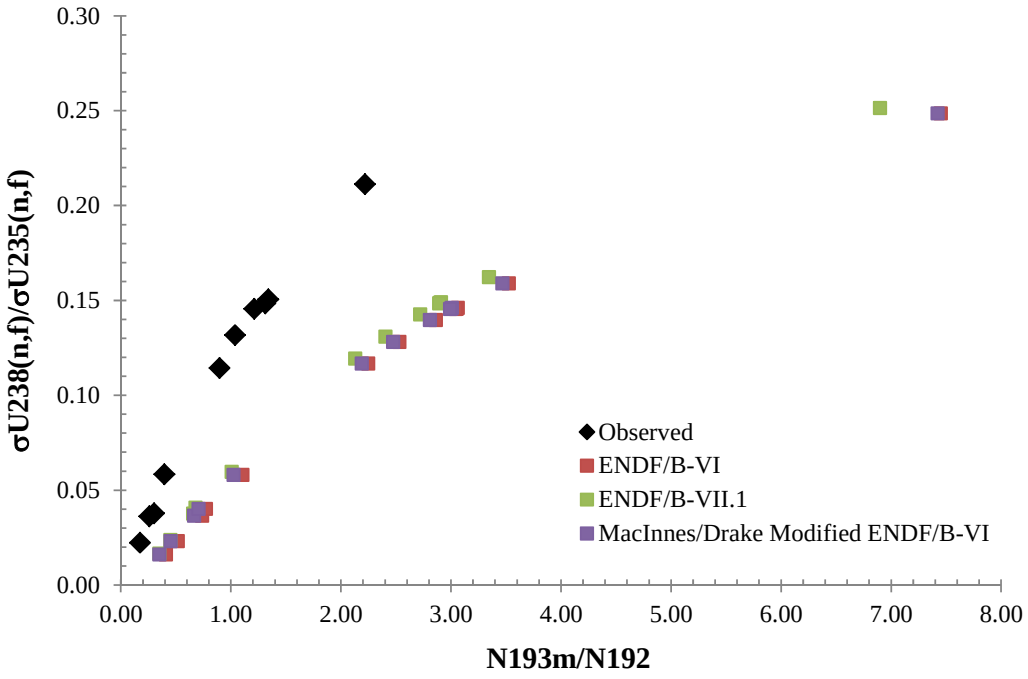

Figure 7-5 Behavior of the uranium fission cross section ratio to the iridium spectral index between the ENDF data and observed data is plotted.

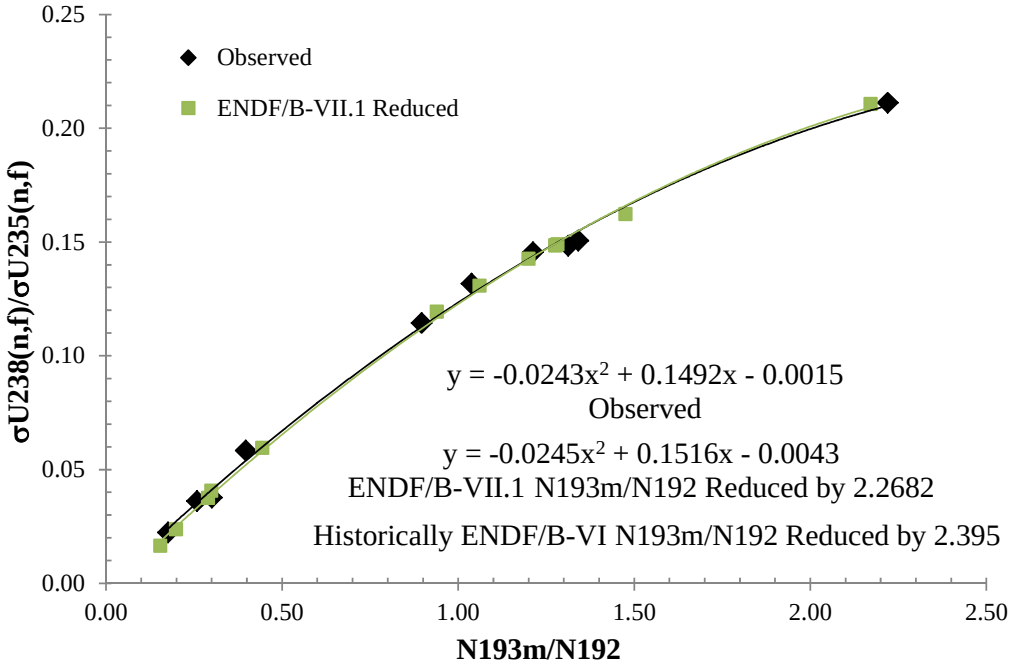

Figure 7-6 Curve fits of the observed data and ENDF/B-VII.1 calculated data is plotted. ENDF/B-VII.1 N193m/N192 data has been reduced by 2.2682 to move the curve to fit to the observed data. Historically the Drake modified ENDF/B-VI data was reduced by 2.395. Calculated virgin data points are not included.

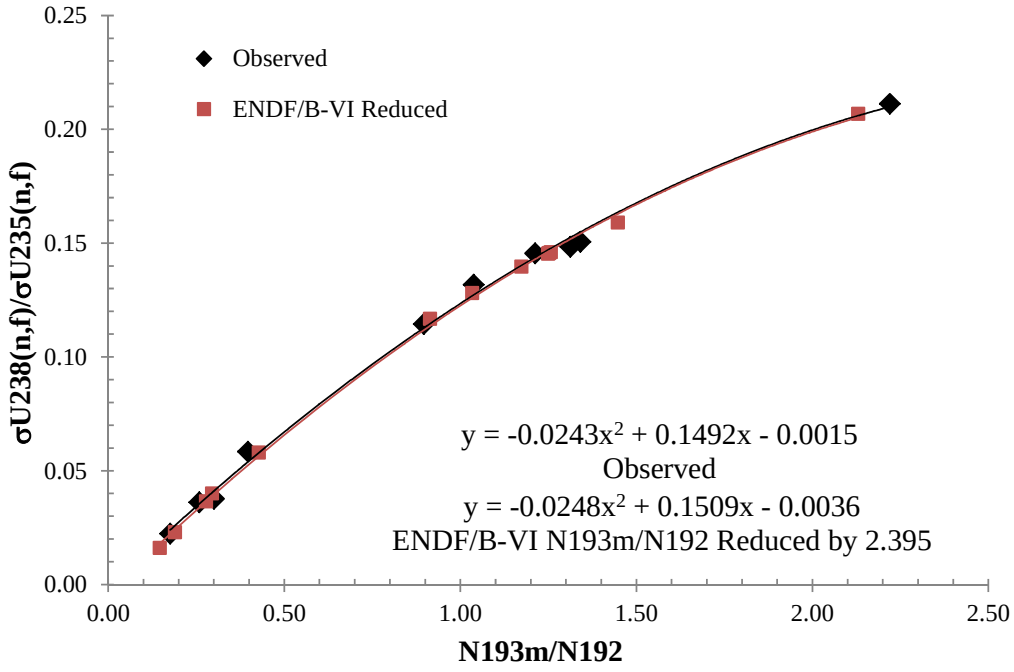

Figure 7-7 Curve fits of the observed data and ENDF/B-VI calculated data is plotted. ENDF/B-VI N193m/N192 data has been reduced by 2.395 to move the curve to fit to the observed data. Calculated virgin data points are not included. Demonstrated is the improvement observed in the fit by using the ENDF/B-VII.1 dataset.

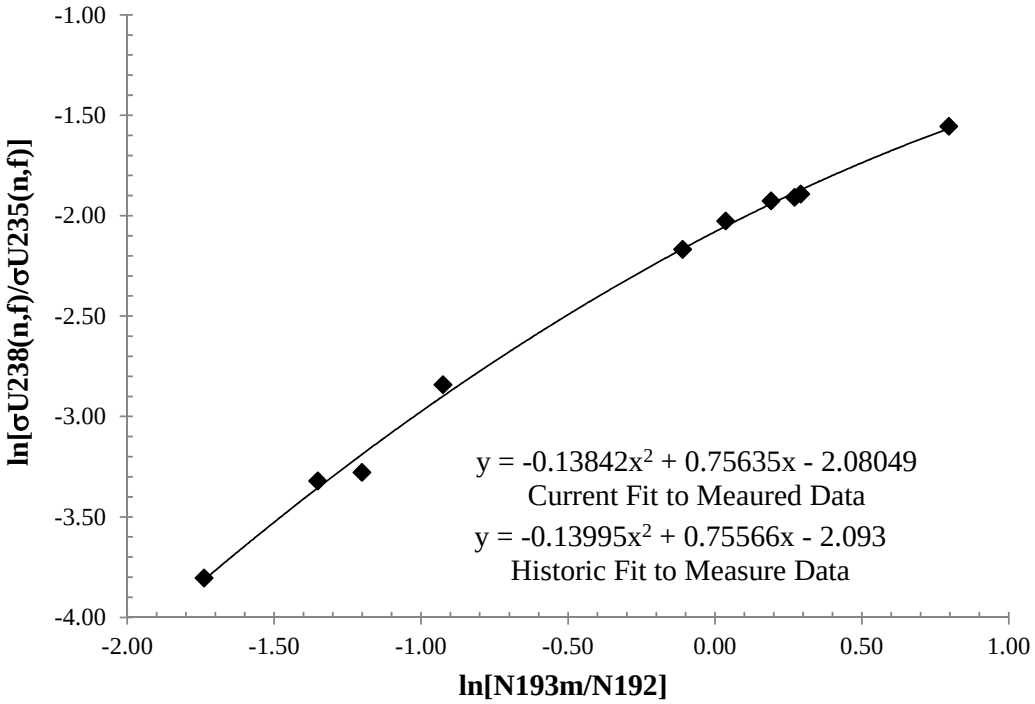

Figure 7-8 Current data fit using re-evaluated measure data with a polynomial function on a log-log scale. Historic fit to measured data is currently used the IPC cross section library.

Table 7-1 Reduced iridium spectral index for ENDF/B-VI and ENDF/B-VII.1 data and calculated relative difference. Applied flux profile is based on the Big-10 critical assembly for ENDF/B-VI results. ENDF/B-VII.1 results applied the appropriate critical assembly flux profile and NJOY weighting function.

	MacInnes/Drake ENDF/B-VI	**ENDF/B-VII.1**	
Critical Assembly	**N193m/N192**	**N193m/N192**	**% Diff**
Virgin Fits Uranium	3.0999	3.0421	1.88%
Godiva	1.4474	1.4752	1.90%
Flattop Oralloy Center	1.2569	1.2827	2.03%
Flattop Oralloy 0.887 cm	1.2524	1.2782	2.04%
Flattop Oralloy 1.131 cm	1.2495	1.2754	2.05%
Flattop Oralloy 3.517 cm	1.1736	1.2000	2.22%
Flattop Oralloy 5.046 cm	1.0341	1.0605	2.52%
Flattop Oralloy 5.718 cm	0.9141	0.9397	2.76%
Flattop Oralloy 8.188 cm	0.4281	0.4444	3.73%
Flattop Oralloy 10.89 cm	0.2779	0.2901	4.32%
Flattop Oralloy 14.67 cm	0.1893	0.1988	4.93%
Flattop Oralloy 20.26 cm	0.1463	0.1543	5.33%
Big-10	0.2950	0.2994	1.47%
Reduction Factor	2.395	2.2682	

Table 7-2 Reduced iridium spectral index for ENDF/B-VI and ENDF/B-VII.1 data and calculated relative difference. Applied flux profile is based on the Flattop critical assembly with a plutonium core for ENDF/B-VI results. ENDF/B-VII.1 results applied the appropriate critical assembly flux profile and NJOY weighting function.

	MacInnes/Drake ENDF/B-VI	**ENDF/B-VII.1**	
Critical Assembly	**N193m/N192**	**N193m/N192**	**% Diff**
Virgin Fits Plutonium	3.3128	3.3175	0.14%
Jezebel Plutonium Core	2.1300	2.1622	1.50%
Flattop Plutonium Center	1.5864	1.6240	2.34%
Flattop Plutonium 0.884 cm	1.5731	1.6108	2.36%
Flattop Plutonium 1.790 cm	1.5311	1.5688	2.43%
Flattop Plutonium 2.697 cm	1.4496	1.4872	2.56%
Flattop Plutonium 3.604 cm	1.3055	1.3424	2.78%
Flattop Plutonium 4.465 cm	1.0336	1.0667	3.15%
Flattop Plutonium 8.354 cm	0.3556	0.3713	4.32%
Flattop Plutonium 12.274 cm	0.2166	0.2276	4.97%
Flattop Plutonium 16.193 cm	0.1603	0.1693	5.44%
Flattop Plutonium 20.113	0.1196	0.1262	5.38%
Reduction Factor	2.395	2.2682	

— 8 — Summary

Summarized in this document is the historical approach used to determine the iridium spectral index for IPC evaluations. The work involved re-evaluating measurement data collected from critical assembly experiments performed between the 1950's and 1970's. A significant amount of effort has been put into to researching the appropriate K-factors utilize at each date the measurement was performed to accurately convert counts to atoms. K-factors are counter dependent and therefore have been variable over the course of the critical assembly experiments performed at LANL due to upgrades and maintenance performed on the counter. Additionally uncertainly has been propagated from counts to K-factors to atoms conversions providing an error estimate on observed data which has not been previously done. As comparison to the historical data the iridium spectral index is determined using the ENDF/B-VII.1 dataset.

A suite of applications have been developed in Python to process ENDF cross section data. These applications are used to perform the collapse on the ENDF data over the LANL 30-group energy bins and determine average cross sections at specified locations in critical assemblies. Accuracy in fitting the ENDF datasets to the observed data is improved in comparison to the historic method by minimizing chi-squared during the analysis. This new application suite will allow for new data to processed and folded into the IPC cross section library with ease. It is now a trivial process to add and remove data points to compare cross section fits.

Measurements of integral cross sections are essential to the determination of the cross section functions used in IPC. Without observed data the calculated cross section from the ENDF libraries cannot be validated. Verified by the work is the bias present in the counting of iridium foils. Observed data currently being utilized are from critical assembly experiments performed from the 1950's to 1970's. New measurements would be of great value for further validation. Determination of the current iridium counting bias is of interest to investigate the application of applying iridium fits based on ENDF data rather solely based on measured data. Modifications between ENDF/B-VI and ENDF/B-VII.1 libraries resulted in an improved fit of the uranium fission ratio and iridium spectral index to the measured data. In addition, cross section fits are adjusted by applying the appropriate weighting functions in the reduction of ENDF data into the LANL 30-group energy bins.

Experiments that include uranium, plutonium and iridium foils at varying location in critical assemblies would strengthen cross section relationships between plutonium and uranium. There are a limited number of experiments performed with a plutonium core and those performed did not always include an iridium measurement. Additional data would be valuable to strengthening the IPC cross section library.

— 9 — Appendix A: ENDF Data

LANL 30-Group structure comparison between critical assembly weighting functions for ENDF/B-VII.1 data for uranium, plutonium and iridium isotopes are given in Figure 9-1 to Figure 9-4. It is evident that the difference between the weight function is not significant.

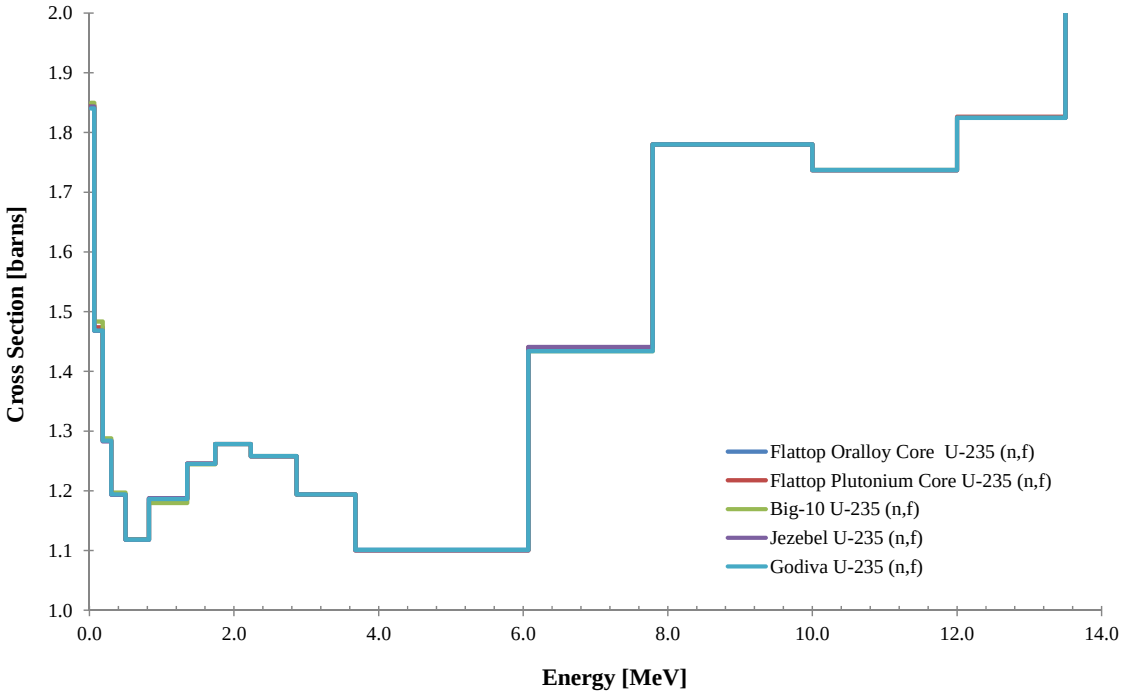

Figure 9-1 Comparisons of LANL 30-Group structures based on weighting functions for the Flattop, Big-10, Jezebel and Godiva critical assemblies using ENDF/B-VII.1 data for the ^{235}U neutron fission reaction.

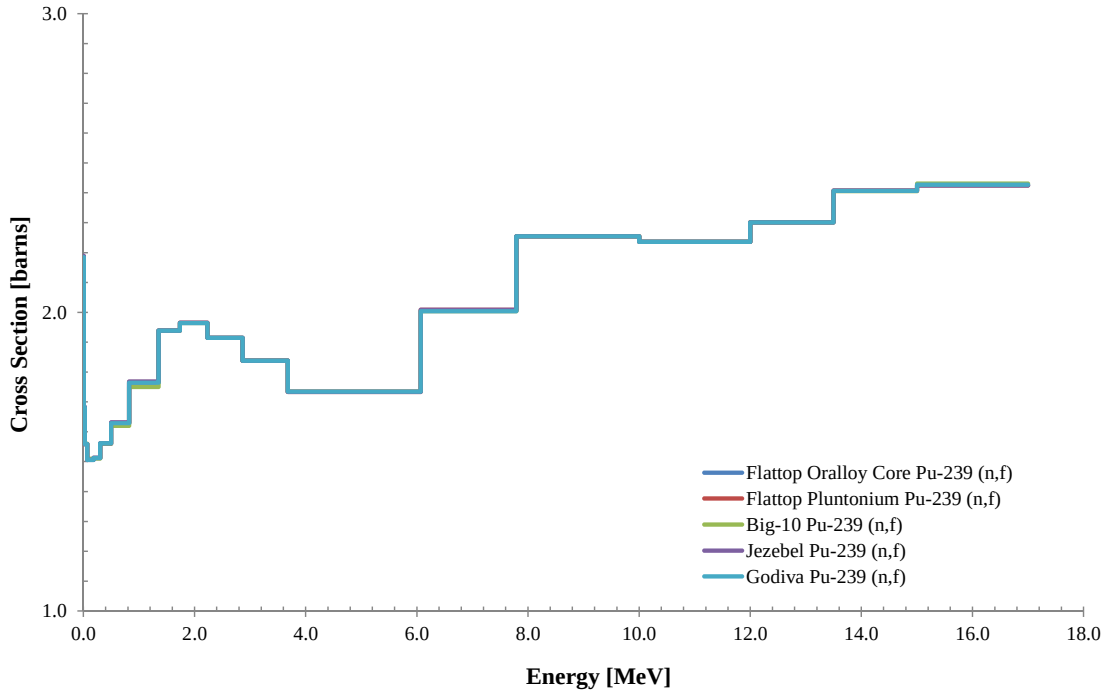

Figure 9-2 Comparisons of LANL 30-Group structures based on weighting functions for the Flattop, Big-10, Jezebel and Godiva critical assemblies using ENDF/B-VII.1 data for the ^{239}Pu neutron fission reaction.

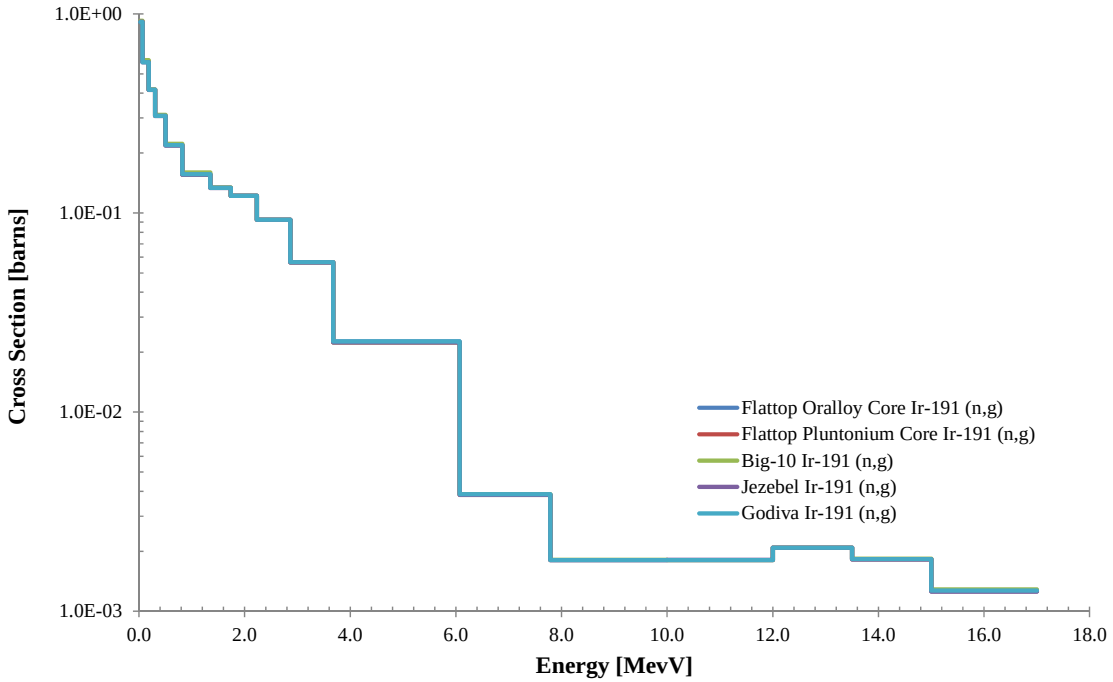

Figure 9-3 Comparisons of LANL 30-Group structures based on weighting functions for the Flattop, Big-10, Jezebel and Godiva critical assemblies using ENDF/B-VII.1 data for the ^{191}Ir neutron capture reaction.

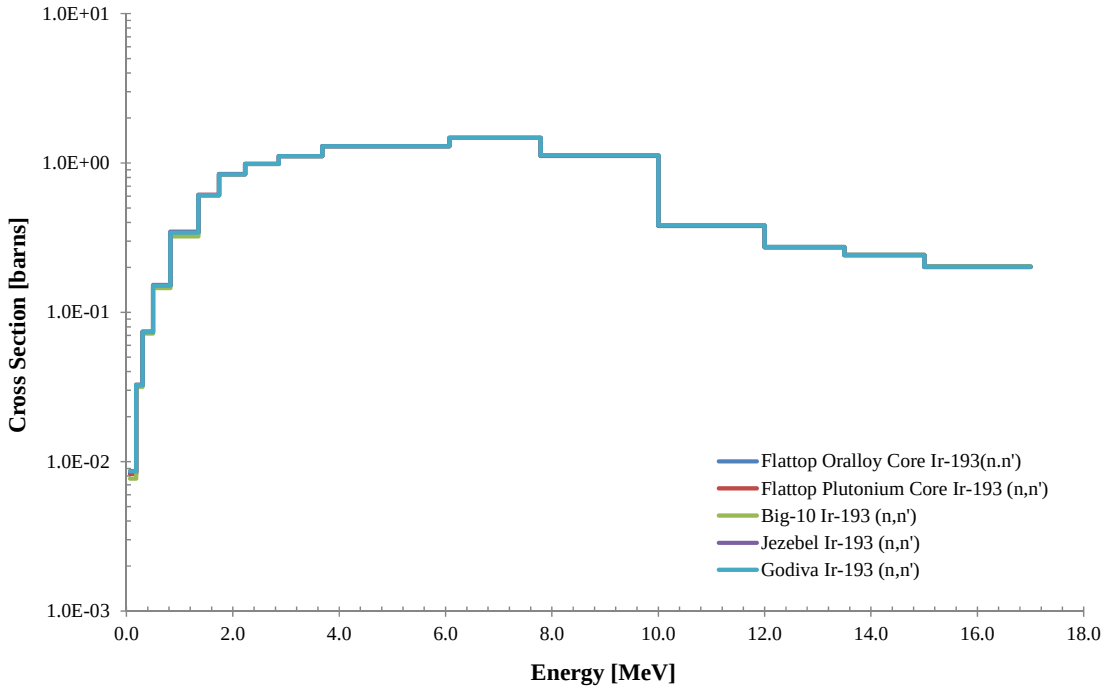

Figure 9-4 Comparisons of LANL 30-Group structures based on weighting functions for the Flattop, Big-10, Jezebel and Godiva critical assemblies using ENDF/B-VII.1 data for the ^{193}Ir inelastic neutron scatter reaction.

— 10 — References

[1] D. W. Barr, Pajarito Irradiations (Laboratory Notebook), Los Alamos, New Mexico 87545: Los Alamos National Laboratory, 1967-1975.

[2] H. Paxton, "A History of Critial Experiaments at Pajarito Site," Los Alamos National Laborratory, LA-9685-H, Los Alamos, NM , March 1983.

[3] G. Perdikakis, C. Papadopoulos, R. Vlastou, A. Lagoyannis, A. Spyrou, M. Kokkoris, S. Galanopoulos, N. Patronis, D. Karamanis, C. Zarkadas, G. Kalyva and S. Kossionides, "Measurement of the Am-241(n,2n) reaction cross sections using the activation method," *Physical Review C*, vol. 73, no. 6, pp. 1-4, 2006.

[4] D. Barr, "Radiochemistry Notebook - LAN-15586," Los Alamos National Laboratory, Los Alamos, New Mexico, 1968.

[5] H. Selby, M. Mac Innes, D. Barr, A. Keksis, R. Meade, C. Burns, M. Chadwick and T. Walstrom, "Fission Product Data Measured at Los Alamos for Fission Spectrum and Thermal Neutrons on 239Pu, 235U, 238U," *Nuclear Data Sheets*, vol. 111, pp. 2891-2922, 2010.

[6] H. Selby, "Thermal r-value Evauation Spreadsheet," Los Alamos National Laboratory, Los Alamos, 2010.

[7] M. Chadwick, "ENDF/B-VII.1 Nuclear Data for Science and Technology: Cross Section, Covariance, Fission Product Yield and Decay Data," *Nuclear Data Sheets*, vol. 112, no. 12, pp. 2887-2996, 2011.

[8] R. MacFarlane and A. Kahler, "Methods for Processing ENDF/B-VII with NJOY," *Nuclear Data Sheets*, vol. 111, pp. 2739-2890, 2010.

[9] M. Mac Innes, Evaluation of US Test Data (INC-11-1361), Los Alamos, NM: Los Alamos National Laboratory, 1992.

[10] J. Schecker, M. Mac Innes, D. Barr, W. Inkret and W. Efurd, "A Re-evaluation of LANL Historic Radiochemistry Constants," Los Alamos National Laboratory, LA-UR-05-3760, Los Alamos, New Mexico, 2005.

[11] J. Schecker, "History of Fission Product Calibrations at Los Alamos," Los Alamos National Laboratory, LA-UR-04-1197, Los Alamos, New Mexico, 2004.

[12] C. Burns, M. S. H. Mac Innes and A. Keksis, "Los Alamos Fission Basis - LANL/LLNL Fission Product Evaluation Review Panel," Los Alamos National Laboratory, LA-UR-09-04489, Los Alamos, New Mexico, 2009.

[13] M. Mac Innes, M. Chadwick and T. Kawano, "Fission Product Yields for 14 MeV Neutrons on U-235, U-238 and Pu-239," *Nuclear Data Sheets*, vol. 112, pp. 3135-3152, 2011.

[14] J. Grundl, D. Gilliam, N. Dudey and R. Popek, "Measurement of Absolute Fission Rates," *Nuclear Technology*, vol. 25, pp. 237-257, 1975.

[15] Cross Sections Evaluation Working Group, "ENDF-6 Formats Manual," National Nuclear Data Center, Upton, NY, October 24, 2012.